Fall 2019

# Development of a Rangeland Degradation Risk Model for the Peruvian Andes

Colin Schmidt
*Western Washington University*, colinrs017@gmail.com

# DEVELOPMENT OF A RANGELAND DEGRADATION RISK MODEL FOR THE PERUVIAN ANDES

By

Colin Schmidt

Accepted in Partial Completion
of the Requirements for the Degree
Master of Science

ADVISORY COMMITTEE

_____

Chair, Dr. John All

_____

Dr. Andrew Bach

_____

Dr. Robin Matthews

_____

Dr. Narcisa Pricope

GRADUATE SCHOOL

_____

David L. Patrick, Interim Dean

## Master's Thesis

In presenting this thesis in partial fulfillment of the requirements for a master's degree at Western Washington University, I grant to Western Washington University the non-exclusive royalty-free right to archive, reproduce, distribute, and display the thesis in any and all forms, including electronic format, via any digital library mechanisms maintained by WWU.

I represent and warrant this is my original work, and does not infringe or violate any rights of others. I warrant that I have obtained written permissions from the owner of any third party copyrighted material included in these files.

I acknowledge that I retain ownership rights to the copyright of this work, including but not limited to the right to use all or part of this work in future works, such as articles or books.

Library users are granted permission for individual, research and non-commercial reproduction of this work for educational purposes only. Any further digital posting of this document requires specific permission from the author.

Any copying or publication of this thesis for commercial purposes, or for financial gain, is not allowed without my written permission.

Colin Schmidt

15 August 2019

# Development of a Rangeland Degradation Risk Model for the Peruvian Andes

A Thesis
Presented to
The Faculty of
Western Washington University

In Partial Fulfillment
Of the Requirements for the Degree
Master of Science

By
Colin Schmidt
August 2019

## Abstract

This study developed a Rangeland Degradation Risk Model for the Peruvian Andes based on the Unit Stream Powered Erosion Deposition Model using globally available datasets. A supervised land cover classification was conducted to identify suitable grazing areas and to conduct a regional analysis of susceptibility to erosion. Field data were collected from two different study sites, Huascaran National Park and Nor Yauyos Cochas Landscape Reserve, and were used to assess the model's accuracy in different ecosystems and land use types. Field data were also leveraged to identify additional data needs and other potential drivers of degradation not taken into account by the model. The accuracy assessment showed that while the Advanced Spaceborne Thermal Emission and Reflection Radiometer Digital Elevation Model (ASTER DEM) was adequate for estimating slope and aspect, data sets used for estimating vegetative cover and soil properties were unable to capture spatial heterogeneity seen in the field. A correlation analysis among field data suggested that topographic forcing was a major driver of degradation, but discrepancies between modelled and observed field condition suggested that the effects anthropogenic factors need to be better accounted for in order to improve the model's accuracy. The integration of a supervised land cover classification with a soil erosion and deposition model allows for areas at risk for degradation due to topographic forcing to be identified for further analysis and monitoring. Additional research is needed to predict soil properties and vegetative cover at a higher spatial resolution to better understand their influence on rangeland condition as well as to further investigate other drivers of degradation.

## Acknowledgements

I would like to thank Samuel Pizarro, Bill Yalli, and Jorge Salinas for their assistance in the development and processing of the Rangeland Degradation Risk Model as well as field data collection and site selection methods. I would also like to thank the faculty, staff, and students at Universidad Agraria La Molina for their hospitality and logistical support. Lastly, I would like to thank the Huxley Small Grant, the Dean's Fund for Sustainability, and the Ross Travel Grant for providing me with the funding needed to complete my fieldwork.

## Table of Contents

## List of Tables and Figures

## Introduction

### Rangelands

Rangelands, which cover 40% of earth's terrestrial surface, are described by the Society of Range Management as native plant communities that are managed ecologically rather than agriculturally (Society for Range Management 2019). In addition to their ecological value, rangelands are a valuable economic resource. Rangelands are commonly used as grazing land for livestock, the world's most common land use practice, as well as for recreational and aesthetic values (Krausman et al. 2009).

Rangeland degradation can be described as a reduction in land quality or productivity due to natural or anthropogenic factors (Eswaran et al. 2001). This can include overgrazing, fire, or climatic changes. Changes in soils, including accelerated erosion or change in composition, are the main driver of physical, chemical, and biological land degradation (Eswaran et al. 2001).

Anthropogenic rangeland degradation can be mitigated by land owners and managers. Rangelands should be managed to optimize the sustained yield of economic and ecological resources. Effective management of grazing lands requires that land use reflects the quality of the land to minimize the negative effects of overgrazing (Milton et al. 1994). This includes soil compaction, loss of vegetation and biodiversity, and accelerated erosion. Rangelands are dynamic ecosystems that lack a single climax state, but have several potential states that can change due to anthropogenic or climactic events (Westoby et al. 1989). Management should reflect these processes and focus on constantly cataloging, monitoring, and assessing rangeland condition to inform management decisions (Westoby et al. 1989). Management actions should be based on spatial distribution of rangeland condition and rate of degradation.

Land managers and researchers alike shape their understanding of the environment through personal experiences and use them to construct a mental template of their reality.

Since the experiences of various stakeholders vary, so do their mental models of rangeland processes (Abel et al. 1998). In order for communication of information between land managers and researchers to be effective, one must understand the concerns and circumstances of the other (Abel et al. 1998). This can be achieved by simplifying the underlying theory and focusing on providing land managers with practical and simple management tools geared toward their needs (Abel et al. 1998).

## Predicting Soil Erosion

The universal soil loss equation (USLE) was developed using several decades of soil erosion data and can be used to empirically estimate erosion rates based on six environmental factors, including land cover, rainfall, soil properties, topography, and support practices (Wischmeier and Smith 1978). Developed by the USDA, USLE and its revisions, known as the revised universal soil loss equation (RUSLE), traditionally have been used for long term estimates of erosion rates to improve management of agricultural lands (Renard et al. 1991).

The Unit Stream Power-Based Erosion Deposition Model (USPED) is a sediment transport model that calculates erosion and deposition rates, expressed in tons/acre/year (Warren et al. 2005). Unlike the RUSLE model, the USPED model spatially delineates sediment deposition as well as erosion by accounting for upslope water movement and sediment transport, making it a favorable model for predicting erosion across topographically complex landscapes (Warren el al. 2005). The USPED model differs from RUSLE in its method of calculating slope length and steepness, or the LS factor (Pricope 2009). The USPED model takes into account the upslope contributing area when calculating the LS factor. Studies that have validated and compared results of the models have shown that the USPED model is more accurate than RUSLE, claiming that the latter overestimated soil erosion (Warren et al. 2005).

Traditionally, erosion models have been used for lumped estimates of erosion rates for large areas. However, recent developments in GIS and availability of high resolution elevation

models and satellite imagery has allowed for soil erosion rates to be assessed at a large scale with greater accuracy (Mitasova et al. 1996).

Unmanned aerial systems (UAS) technology in the last decade has improved the efficiency of the collection of high resolution aerial imagery. These new advancements in remote sensing can reduce the cost and time required to collect high resolution data in large areas or remote places. UAS technology has the potential to improve monitoring, modelling, and assessment of heterogeneous areas when the resolution of globally available datasets are not sufficient. High resolution data collected by UAS can also be used for determining plant structure and biodiversity, assessing human impacts, and constructing high resolution digital elevation models (Gallacher 2015).

## Study Area

The Andean puna lies at an elevation between 3,500 and 5,500 meters and covers over 100,000 square kilometers stretching from southern Peru to northern Bolivia. The primary ecosystems are upland grasses and wetlands in valley floors (Baied and Wheeler 1993). The dry puna averages just 30 to 50 centimeters of rainfall annually, which limits the vegetation to primarily grasses and shrubs. This lack of rainfall and cold temperatures limits agriculture to below 4,000 meters (Baied and Wheeler 1993).

Bofedales are wetland plant communities located in the Peruvian Andes characterized by constant, year-round humidity, and can be indicated by the presence of peat or organic soil (Fonken 2014). Bofedales are generally located in riparian floodplains and are an important component in the movement of water in these highlands. They receive water from glacial melt, groundwater, or rainfall at higher elevations, and store and regulate the movement of water downslope. Drenkhan et al. (2015) discusses the fragility of these ecosystems, asserting that climate change can accelerate fragmentation of these ecosystems and alter water storage in the area.

Andean ecoregions provide many valuable ecosystem services. Most importantly, glaciated regions of the tropical Andes are an essential water source for surrounding communities (Drenkhan et al). In the Andean puna, bofedales are an important aspect of highland grazing, as they provide a reliable source of food and water to grazing animals and the surrounding communities. Grazing in the Peruvian Andes is an essential part of the economies of Andean countries, as the vast majority of grazing animals in high Andean regions are located in Peru (Millones 1982).

Semi arid rangelands are fragile ecosystems that are particularly susceptible to projected climate change scenarios. Projected changes in temperature and precipitation will alter habitat of endemic high Andean and may result in accelerated desertification and a loss of biodiversity (Feely and Filman 2010). It may also adversely affect quality of soils by increasing decomposition rate of organic matter and altering soil structure (Kumar and Das 2014). Semi arid rangelands are complex ecosystems, and their response to climate change is difficult to predict. Furthermore, uncertainties in future temperature, rainfall patterns and land use pose many challenges for land managers.

Much of the puna is used as grazing land for llamas, alpacas, cattle and sheep. According to Millones (1982) there are an estimated 19 million hectares of naturally occurring grazing land in elevations above 2,500 meters. In contrast to llamas and alpacas, cattle and sheep pose a much greater threat to rangeland degradation. The hooves of sheep disrupt the fragile groundcover, unlike llamas and alpacas padded feet. Sheep also eat plants down to the root, whereas llamas and alpacas are able to clip off the desired part without disrupting the root structure (Baied and Wheeler 1993).

The majority of grazing livestock are owned either by small communities or families, known as campesino communities. Around one third of Peru's grazing land is held in cooperative institutions known as Sociedad Agricola de Interes Social, or SAISs, which generally have a much lower stocking rate and are better managed than community held lands

(Lodaza 1991). It is estimated that the number of grazing animals in Peru exceeds the amount that can be supported by the land by 17% (Lozada 1991). The use of technology is limited in most grazing and agricultural communities. They rely primarily on human and animal labor for herding, planting, and harvesting and use compost or manure as fertilizers (Millones 1982).

## Huascaran National Park

The Cordillera Blanca is the highest tropical mountain range in the world and is protected by Huascaran National Park, which cover 3,400 $km^2$ (UNESCO). It is located north of Lima in the Ancash province of Peru (Figure 1). The region's climate is largely dependent on altitude, with an annual average temperature of 18 C in the valleys and below 0 C in the highest areas, and receives 770 mm of annual precipitation in the north and 470 mm annually in the south (UNESCO).

While the park itself is home to less than 1,000 people, the surrounding buffer zone, which encompasses an additional 5,710 $km^2$, is home to 226,500 people (Byers 2000). Nearly three quarters of these people live in rural campesino communities, relying on subsistence agriculture and cattle grazing to maintain their livelihood (SERNANP 2012, Byers 2000). The cultural practices of these communities and their dependence on communally held land has been recognized in the management plan for Huascaran National Park (SERNANP 2012). Campesino communities have been granted the right to continue to use park lands for cattle grazing in designated special use zones, primarily in the low lying pastures including those in Ulta and Quilcayhuanca valleys (SERNANP 2012).

Overgrazing in these pastures has led to increased soil erosion, compaction, and a loss of vegetation, as the number of animals grazed has exceeded the land's sustainable carrying capacity (SERNANP 2012).

The main population centers are located to the west of the Park and include the city of Huaraz and Caraz, which hold 90,000 and 15,000 people respectively. Huaraz is the tourism hub for the park and sees over 100,000 visitors annually (Byers 2000).

The proposed soil erosion model was applied to the Ulta and Quilcayhanca valleys in Huascaran National Park (Figure 2). The two respective drainage basins are delineated below using an ASTER digital elevation model from 2011 and the hydrology toolset in ArcGIS.

Nor Yauyos Cochas Landscape Reserve

The Nor Yauyos Cochas Landscape Reserve covers over 221,000 hectares in the foothills of the Peruvian Andes and is located in the provinces of Yauyos and Jauja (Shoobridge 2005). It was created in 2001, but has no on site land managers or rangers, and no plan was immediately put in place to manage the area (Shoobridge 2005). The most recent management plan, put into place in 2016, has environmental, economic, and social components that focus on restoring the ecosystem to 2014 conditions as well as promoting sustainable tourism in the area (Shoobridge 2005).

The landscape reserve has a population of 5,550 people. Since agriculture becomes impractical at high altitudes, communities in this regions rely primarily on grazing animals. The landscape reserve is home to 6,750 cattle, 89,200 sheep, 13,000 alpacas, 3,700 llamas, and 200 vicunas (Shoobridge 2005). Two campesino communities within the park, Thomas and Canchayllo, were used as study sites to implement and analyze the rangeland degradation risk model (Figure 3).

**Methods**

The Rangeland Degradation Risk Model was created based on the USPED model using GIS. This model attempted to spatially delineate rate and volume of sediment flux as well as erosion and deposition rate. These values were then used as a basis for assessing risk for rangeland degradation. The USPED model is based on the Revised Universal Soil Loss Equation, which calculates annual average soil loss (ASL) using the equation

$$ASL=R*K*C*P*LS$$

where R is rainfall erosivity, K is soil erodibility, C is land cover management, P is support practices, and LS is slope length and steepness (Renard et al. 1991). The USPED model replaces the LS factor to account for upslope contributing area, making it a favorable model for computing soil erosion and deposition rates at the landscape scale (Pricope 2009). The USPED model calculates relative erosion and deposition rates using the following equation:

$$ED = div\ (qs) = d(qs \cos a)/dx + d(qs \sin a)/dy$$

where a is the aspect angle and

$$qs=R*K*C*P*A^{m}\sin^{n}b$$

Model inputs are derived from the sources shown in Table 1 and are described below.

Rainfall Erosivity (R Factor)

The rainfall erosivity factor measures the erosive effect of precipitation amount and intensity. It takes into account both the detachment of soil particles from raindrop impact as well as the rate and volume of soil movement from surface runoff (Renard et al. 1991). Traditionally, the R factor value is derived from the EI parameter, calculated by multiplying the total storm energy by the maximum 30-minute precipitation rate in inches per hour (Renard et al. 1991). In order to accurately derive this value, it is recommended that precipitation intensity data be used from at least 22 consecutive years (Renard et al. 1991). Nor Yauyos Cochas and Huascaran National Park lack sufficient rain gauge precipitation data, so alternative ways of estimating rainfall erosivity were used. The R factor was calculated using Climate Hazards Group InfraRed Precipitation with Station (CHIRPS) data. The CHIRPS program uses infrared satellite data to estimate monthly precipitation from 1981 to 2017 at a scale of 0.05° (Funk et al. 2015). This information can be particularly useful in areas where weather stations are sparse.

The CHIRPS data were analyzed using Python scripts derived from tools in ArcMap. The global monthly CHIRPS data sets were clipped to the study area. The datasets were resampled to the size of a Landsat pixel as well as a MODIS pixel to allow the model to be run at two different scales. Annual average precipitation was calculated by averaging the annual rainfall values from 1981 to 2017. Averages of each month for the same years were used to calculate monthly precipitation averages. These values were entered into the equation

$$F=SUM((\text{Monthly Precipitation})^2/(\text{Annual Average Precipitation})$$

The Modified Fournier Index (Renard and Freimund 1994) was used to calculate the R factor for the study areas with the processed CHIRPS data as inputs. The Modified Fournier Index was developed to calculate rainfall intensity using monthly and annual precipitation data, and is particularly useful when detailed rainfall data are unavailable (Renard and Freimund

1994). Previous studies have shown that the Modified Fournier Index has a strong linear correlation with rainfall erosivity (Renard and Freimund 1994). The Modified Fournier Index values were transformed to reflect R factor values using the equation

$$R=3.82F^{1.41}$$

Soil Erodibility (K Factor)

Soil erodibility can be described as the amount of soil loss per unit of energy applied. This value is influenced by properties of the soil, and several equations attempt to draw a relationship between soil properties and K factor values (Renard 1997). One equation, developed from a database of global soils, uses mean particle size, derived from sand silt and clay percentages, to estimate K factor values. However, this equation can only be used for soils with less than 10% rock fragments.

The K factor was calculated using soil information from the International Soil Reference and Information Center (ISRIC). The ISRIC has recently developed SoilGrids, an information system of predicted global soil properties at various depths based on machine learning (Hengl et al. 2017). Among other properties, SoilGrids includes surface percentage of sand, silt, and clay at a 250 square meter resolution. These values were used to calculate the mean particle size of the soils using the equation

$$Dg=\exp(0.01(\mathrm{SUM}(fi \ln m))$$

where fi is the particle size fraction and m is the mean particle size for clay, silt, and sand. The m values used for clay, silt, and sand were 0.001, 0.026, and 1.025 respectively (Renard et al.

1991). The mean particle size value (Dg) was entered into the equation below to derive the K factor.

$$K = 7.594\left\{0.0034+0.0405\exp\left[-\frac{1}{2}\left\{\frac{\log(Dg)+1.659}{0.7101}\right\}^2\right]\right\}$$

Land Cover Management (C Factor)

Land cover management can be defined as the ratio of soil loss under a certain plant cover type to the amount of soil loss on bare soil. This value, which ranges between 0 and 1, accounts for the prevention of detachment of soil particles due to vegetation cover (Renard et al. 1991). The C factor can be broken down into several sub-factors to estimate the soil loss ratio. These factors include cropping impacts, vegetative canopy, and surface cover (Renard et al. 1991). The Normalized Differential Vegetation Index (NDVI) is calculated using the infrared and near-infrared reflectance using the equation (NIR-Red)/(NIR+Red) and is an indicator of vegetation health and productivity (Durigon et al. 2014). NDVI is a ratio of radiant energy emitted by vegetation to the total energy emitted from the vegetation contained within a pixel, and has been used in previous studies as a way to estimate the cover management factor (Erencin 2000, Durigon et al. 2014).

The NDVI values were calculated from both MODIS and Landsat imagery. A composite raster dataset was created using maximum NDVI values derived from Landsat imagery from the dry season (April to November) in the years 2014 to 2018. A maximum value composite was also created from MODIS imagery from the years 2015 to 2018.

The NDVI values were normalized to estimate percent cover of green vegetation ($F_g$) as described by Gutman and Ignatov (1998). The NDVI values corresponding to bare soil

($NDVI_{bare\ soil}$) and fully vegetated areas ($NDVI_{vegetated}$) are used to more accurately reflect vegetative cover for the specific study area. These values were used to calculate percent of vegetated cover using the equation:

$$F_g = NDVI\text{-}NDVI_{bare\ soil} / NDVI_{vegetated} - NDVI_{bare\ soil}$$

Values for $NDVI_{vegetated}$ and $NDVI_{bare\ soil}$ were derived from a previous study that compared field plot data to NDVI values for bare and vegetated areas in the High Andean rangelands (Pizarro 2017). Values of of 0.1275 for bare soil and 0.63 for fully vegetated areas were used for the FCV calculation.

All resulting values greater than 1 were set to 1, and all values less than 0 were set to 0. The fraction of green vegetation map was transformed to reflect C factor values using the equation (1-NDVI)/2.

Two iterations of the model were run with two different inputs for the C factor. The first used Landsat imagery, which has a scale of 30 meters, and the second used a MODIS maximum value composite, which has a scale of 250 meters. This allows for the model results to be compared at two different scales. All other factors were resampled to match the C factor layer resolution. The MODIS maximum value composite was derived by calculating the maximum value for each pixel from MODIS for the years 2015 to 2018, and was used as the input for the above C factor equation.

Slope Length and Steepness (LS Factor)

Slope length and steepness were derived from an Advanced Spaceborne Thermal Emission and Reflection Radiometer Digital Elevation Model (ASTER DEM). This sensor, developed by the United States and Japan, has been collecting high resolution multispectral imagery from NASA's Terra satellite since 2000 (Tachikawa et al. 2011). Validations of the elevation model

showed that the most recent version of the ASTER DEM had a root mean square error of 6.1 meters when compared to geodetic references (Tachikawa et al. 2011)

The LS factor was calculated with the ASTER DEM using the equation $A^m \sin^n b$, where b is the surface slope in degrees and A is upslope contributing area (Pricope 2009). m and n are coefficients to account for prevailing erosion type, and were set to 1.6 and 1.3 for prevailing rill erosion (Pricope 2009).

Model Processing

A supervised land cover classification was conducted in ENVI to identify areas that were suitable for grazing, as these will be the main focus of the analysis. Regions of interest (ROIs) were collected at the study sites in Nor Yauyos Cochas and Huascaran National Park, which included information on ground cover type and vegetation structure. These ROIs were collected by Laboratorio de Ecología y Utilización de Pastizales at the National Agrarian University in Lima, Peru in 2016 and have nearly 650 training sites. They contain data on land cover and vegetation structure. These ROIs were used to identify areas of Landsat Imagery from July 2017 with similar spectral signatures throughout the entire study area. They were then classified as tallgrass, shortgrass, bofedales, water, snow, bare rock, bare soil, forests, or moraine.

Lands were classified based on elevation, humidity regime and the land cover classification mentioned above. An ASTER DEM was used to create four different elevation classes. The elevation classes used were 3,500-4,000 meters, 4,000-4,500 meters, 4,500-5,000 meters, and > 5,000 meters. Humidity regime was divided into five classes and was derived from an ecological map developed by the Peruvian National Office for the Evaluation of Natural Resources (ONERN 1976).

After these three classifications were combined into one ecosite map, a mask was created to eliminate areas that are not suitable for grazing. This included developed areas,

such as urban or mining areas, unvegetated areas, and areas with slope greater than 60%. Small polygons were then aggregated to nearby larger ones, and ecosites smaller than 4 hectares were filtered out. The resulting map predicts areas within the study site that are suitable for grazing (Figure 4). This map was used to inform field sampling locations to assess the accuracy of the model.

Rangeland Degradation Risk Model

The results of the USPED model using Landsat imagery for the C factor were used to conduct an assessment of erosion and deposition rates for each ecoregion suitable for grazing using the land cover classification map. For Nor Yauyos Cochas, the same assessment was conducted using the watersheds within the study area. Assessing erosion and deposition by region or watershed will make it easier to identify grazing areas at risk of degradation and will also facilitate communication with land managers. The USPED model results using landsat imagery were separated into two different layers, one representing erosion (negative values) and one representing deposition (positive values). The sum of these two layers was then calculated separately for each ecosite and watershed. These values were used to create a ratio of deposition to erosion. Values greater than one indicate higher rates of deposition, and values of less than one indicate higher values of erosion. These values can be used to assess the severity of landscape change in each ecoregion as well as within each watershed.

A supervised classification was conducted based on the results of the erosion to deposition ratio calculated for each watershed and ecosite. Natural breaks were used to separate the data into three classes, one to represent areas of predominantly high erosion, one for areas of predominantly high deposition rates, and one for stable areas.

## Field Methods

Data on slope, aspect, elevation, land cover, vegetation, and soil properties were collected in the field and were used to assess the accuracy of each of the model inputs. This allowed for potential sources of error to be identified.

Fieldwork was conducted in two campesino communities in Nor Yauyos Cochas Landscape Reserve, Thomas and Canchayllo, and in Ulta and Quilcayhuanca Valley in Huascaran National Park in July and August of 2018. Additional ground control points were taken in October of 2017 in Nor Yauyos Cochas. The goal of this work was to collect data on the physical characteristics, vegetation, and ecosystem health to inform and ground truth a soil erosion model for the area. These data were also used to assess correlations of site properties to better understand drivers of rangeland degradation.

## Data Collection

A total of 93 ground control points were collected to use for analysis. Thirty ground control points were collected in Tomas and 30 were collected in Canchayllo in July. An additional 33 points were collected in October of 2017, 18 in Canchayllo and 15 in Thomas. Sampling locations were selected based on the ecosite map created for the study area. Within each ecosystem, replicate points were taken to represent varying rangeland conditions within each ecosystem. The location and elevation of each point along with the associated error was collected using a Garmin 60CS GPS. The points collected had an average error of 6 meters. Slope and aspect were measured with a clinometer and a compass, respectively. Percent land cover, including percentage of grasses, shrubs, water, and soil, were visually estimated and recorded in the surrounding area within a 10 meter radius. The species present were recorded and photographed in order of dominance. Condition of the rangeland was assessed based on the visual impacts of soil erosion and grazing. Panoramic photos were taken of each point. Soil

samples were collected and labelled for select sites. A total of 35 soil samples were collected and analyzed for particle size distribution as well as percent of organic matter.

### Data Analysis

Kendall's rank correlation analysis (**R version**) was conducted for each individual model input that had corresponding field data. This includes MODIS and Landsat derived vegetative cover, soil properties, slope, aspect, and elevation. The absolute mean error was calculated for each model input and corresponding field dataset to determine at what scale each input is accurate to. Finally, the model and field data were plotted to identify systematic biases.

A correlation analysis was also conducted among data collected in the field to better understand how they relate to one another. This can provide valuable information on potential drivers of rangeland degradation.

## Results

### Model Processing

The sediment transport rates given by the USPED model for both Ulta and Quilcayhuanca valleys showed a similar spatial distribution. High rates of deposition were located in valleys, with the highest concentration being where the main rivers flow out of the valleys. High rates of erosion were seen in the steeper slopes surrounding these valleys (figure 5). This pattern is easily visible in Quilcayhuanca valley, as the watershed is dominated by one river that trasects the entire valley. Although Ulta valley has several different basins feeding into the main river, the same pattern was still visible at a slightly smaller scale. The USPED results modelled at the MODIS scale had a similar spatial distribution to the Landsat resolution for both valleys (figure 6). The main difference seen was that the river basins are relatively stable, whereas the

surrounding slopes had high rates of erosion. This is most likely a result of the coarser spatial resolution.

The topography of Nor Yauyos Cochas differs from the valleys of Huascaran National Park in that the landscape is composed of gradual rolling foothills rather than being dominated by larger mountains and glacial valleys. However, a similar spatial pattern was seen at a smaller scale with areas with high rates of deposition concentrated around major rivers within the study area (Figure 7). This pattern was more easily visualized at the MODIS scale, particularly in the rivers in the southwest portion of Thomas (Figure 8).

Both MODIS and Landsat scale model results showed a similar spatial pattern in relation to topography. High rates of erosion were seen on steep hillslopes, whereas high rates of deposition were seen in valleys and river basins. However, MODIS scale results showed larger concentrations of areas with low sediment transport rates. While these were also present in the Landsat scale model results, they were distributed more evenly amongst areas with higher erosion or deposition rates. This can be seen when comparing the two scales in the north and central portion of Canchayllo and the eastern portion of Thomas. At the MODIS scale, these areas were dominated by very low sediment transport rates, whereas the Landsat scale showed a uniform distribution of high erosion, high deposition, and rates near zero. This were most likely due to the higher resolution model being able to discern and calculate erosion rates on smaller topographical features.

While having higher resolution sediment transport information may be more desirable, all model inputs should show an acceptable level of accuracy at the determined scale in order for the given rates to be meaningful. It is also important to consider the needs of land managers and to summarize the information given by the model in a way that relates to their information needs.

The supervised land cover classification in Nor Yauyos Cochas resulted in 22 different cover types in the two study areas, covering 32,931 hectares or 57% of the two study areas.

Shortgrass and tallgrass made up 29% and 24% of the study area respectively, while bofedales made up just 4.3% (Figure 9). Canchayllo is characterized by large uninterrupted ecosites suitable for grazing as seen in the image in Figure 10. The northern part of the study area was predominantly shortgrass whereas the southern portion was mainly tallgrass. The majority of the bofedales were located in the southwest portion of the study area. Grazing areas in Thomas were much smaller in size and were segmented by the complex topography of the area, including steep hillsides and rocky outcrops. The photograph in Figure 11 was taken in the southwest portion of the park, and is a visual example of the topographic features that segments rangelands. Bofedales were more frequent and more uniformly distributed throughout Thomas.

In Ulta and Quilcayhuanca valleys, the land cover predicted by the supervised classification seemed to be largely dependent on elevation. Areas of lower elevation were dominated by bofedales, shrubs, and tallgrasses (Figure 12). Shortgrass dominated higher elevation areas along with polylepis, a high elevation shrub. The photograph in Figure 13 shows how land cover changes with an increase in elevation. The low lying areas surrounding the rivers were bofedales and store most of the water. The surrounding slopes were composed of shortgrass, tallgrass, shrubs, and bare rock and soil depending on elevation and slope.

The tallgrass ecosites in the southeast portion of Canchayllo were mainly classified as stable after the erosion deposition analysis was conducted and the values classified into categories. The northeast portion of Canchayllo, dominated by shortgrass, was predicted to be an area of high erosion. Nearly all classified deposition areas were relatively small ecosites located adjacent to major rivers (Figure 14). Compared to Canchayllo, there were more erosion prone ecosites in Thomas. A high concentration of them were located in the river valleys in the western portion of the park. There were also many erosion classified areas on the northeast border of the study area.

The observed rangeland condition for each ground control point was compared to the ecosite condition predicted by the Rangeland Degradation Risk Model (Table 3). The location of the ground control points in relation to the predicted rangeland condition can be seen in Figure 15. 91.4% of the ground control points collected were located in areas that were predicted to be suitable grazing areas, and the majority of the points outside of these areas were in poor or very poor condition.

The vast majority of points observed to be in very poor condition were located in ecosites predicted as erosion areas, suggesting that areas prone to erosion are at greater risk of rangeland degradation. Figure 16 Shows an ecosite in the southeast portion of Thomas predicted to be an area of erosion. The corresponding photograph, taken from point 44, shows the effects of topography on vegetative cover and rangeland condition on the surrounding hillsides.

Nearly half of the points in stable ecosites were in poor condition, while the other half were in either regular, good, or excellent condition. Since erosion rate is mainly a function of topography, stable ecosites are usually located in flatter areas. While this minimizes the effects of erosion on land degradation, these easily accessible areas are prone to overgrazing, which may help explain the high concentration rangelands in poor condition in these ecosites predicted to be stable. Figure 17 shows an example of an ecosite predicted to be stable which was observed to be in poor condition. Effects of fire as well as grazing sheep can be seen in the nearby area. These anthropogenic factors, not directly accounted for in the model, may contribute to a decline in rangeland condition not attributable to erosion rate.

The results of erosion and deposition analysis by ecosite were also compared visually to ground control points to better understand how rangeland condition varies spatially. Figure 18 shows two points taken in a shortgrass ecoregion. One point is taken at the base of a valley and one taken on the steep hillslope. The latter point has large areas of bare soil and rock from accelerated erosion. Footpaths from grazing animals can be seen on the hillslope. A visual

comparison of the soil at the two sites shows that the steep hillslope has a higher concentration of large particles whereas the area at the base of the valley is composed of finer sediment (Figure 19). This is a visual example of how topography can alter soil properties over a relatively small area.

Classification of erosion rate by ecosite for Huascaran National Park was similar to the spatial distribution seen in Nor Yauyos Cochas. However, since each study site is transected by one main river and there in less complexity in the distribution of ecosites, the pattern can be seen on a much larger scale (Figure 20). Areas of deposition are seen in the low lying areas surrounding the rivers. Although areas at mid elevation are classified as stable, I would hypothesize that it would be more accurate to categorize them as erosion prone areas. The rate of deposition in reality would most likely be lower than the value given by the model, as it fails to account for the large areas of glacier and bare rock that dominate the higher elevations. Visible effects of erosion can be seen in an area classified as stable in Figure 21.

The modelled rates of erosion and deposition given by the USPED model using Landsat imagery for Nor Yauyos Cochas were analyzed for the relative effects of different driving factors. Four different iterations of the model were calculated. Sediment transport rate was calculated as a function of topography, topography and soil erodibility, topography soil erodibility and land cover, and topography, soil erodibility, land cover, and precipitation. Since the output sediment transport rate is a unitless value, the results of the model were standardized by calculating the z-score (value-mean/standard deviation). The resulting histogram can be seen in Figure 22.

The addition of the soil erodibility factor and land cover factor reduced areas with high erosion and deposition values. The area of Z score values between -1 and 1, which are relatively stable values, increased with the addition of these factors. The more extreme values representing higher erosion or deposition rates decreased when soil erodibility and land cover were added. The addition of precipitation had the greatest effect on the distribution of values. Values representing high rates of erosion and deposition saw the most dramatic increase,

whereas the majority of values representing lower erosion and deposition rates reduced in area. The distribution of values between the topographic forcing model and the model containing all four factors are the most similar, suggesting that erosion rate is primarily a function of topography.

## Accuracy Assessment

The slope and aspect data for both study sites were derived from a 30 meter ASTER DEM. The measured slope was significantly correlated with slope values derived from the DEM and had a mean error of 5.93 degrees. This is consistent with the average error of the GPS used to collect the ground control points as well as the error associated with the ASTER DEM. A visual analysis of the relationship between measured and derived values shows that the measured values are consistently less than those derived from the DEM (Figure 23). This may be due to biases in field slope measurements.

The measured and derived aspect values display a strong linear relationship, with the exception of values approaching 360 and values approaching 0 (Figure 24). The mean error was 75 degrees, which may be an overestimation as the error of misclassified values around 360 or 0 degrees is not accurately accounted for in this calculation. Regardless, the two datasets had a significant relationship.

Percentage of vegetated cover measured in the field and estimated vegetation cover using fractional cover vegetation (FCV) were significantly correlated but showed little meaningful relationship (Figure 25). Based on a visual analysis of the plotted results, the landsat derived vegetation data failed to capture the variability in vegetative cover seen in the field. The mean error between the two was 67 degrees, which is inadequate for providing meaningful information for land cover. MODIS fractional cover vegetation and vegetative cover measured in the field showed little linear relationship, and had a mean error of 66.44 percent (Figure 26). Within pixel variability makes it difficult to accurately predict vegetative cover at the individual pixel scale.

However, these data can be useful in conducting regional analysis of vegetative cover to identify suitable grazing lands.

None of the soil properties measured in the field were significantly correlated with estimated soil properties from ISRIC (Figure 27). The variation seen in organic matter and soil composition in the field at the surface level was not accounted for in the estimated data set. The discrepancies between the field data and derived data for soil and vegetation properties could be attributed to within pixel variability. The estimated dataset used is not based on collected field data, but on machine learning, and captures on average 61% of the variation in soil properties at a scale of 250 meters (Hengl et al. 2017). Previous studies have shown that soil properties in semi arid rangelands vary significantly among cover types, and that grazing further increases spatial heterogeneity (Stavi et al. 2008). Based on this information, it would be expected that the ISRIC data would not account for all of the spatial variability in soil properties seen in the field.

Field Data Correlation Analysis

Although some of the modelled datasets do not accurately reflect field conditions at the desired scale, looking at relationships within field data can give valuable information for predicting field conditions and better understanding drivers of rangeland degradation.

For the dataset including all points from Huascaran National Park and Nor Yauyos Cochas, slope was negatively correlated with herb percent, water percent, and rangeland condition (figure 28). Slope was also positively correlated with percent rock. This is consistent with the visual assessment of the images from both parks in figures 11 and 13. Flat areas at the base of the valley are the main area of water storage and are rich in organic matter. On the surrounding steeper slopes, vegetative cover appears to be thinner, and areas of exposed rock or eroded soil are visible on steeper slopes. The negative association with rangeland condition suggests that these steep areas are particularly vulnerable to degradation due to accelerated

erosion rates. These results are consistent with the analysis of the model's driving factors, showing that erosion and deposition rates are primarily a function of topographic forcing.

Slope, herb and soil cover were all significantly correlated with rangeland condition. Condition was positively correlated with herb cover and negatively correlated with slope and soil cover. This suggests that degraded ecosystems can be characterized by larger percent areas of soil and occur on areas with steeper slopes, as these areas are more vulnerable to erosion. Although herb cover is positively associated with rangeland condition, condition is largely dependent on the type of plant, as a rangeland dominated by noxious or invasive plants would be considered to be in worse condition than one dominated by species that are desirable to grazers. Further research is needed to develop a method of predicting vegetation type and structure using remotely sensed data.

Several inconsistencies were seen when separating the data and running a correlation analysis for each park separately (figure 29 and figure 30). Nor Yauyos Cochas has more significant correlations with elevation than Huascaran National Park, the most notable being percent herb and percent soil. I would expect the opposite to be the case, as the land cover classification for Huascaran National Park suggested that land cover type was largely dependent on elevation. This may be due to the fact that samples were collected mainly in lower elevation grazing areas, leaving out bare rock and glaciated areas from the field data set.

A separate analysis was conducted by using only ground control points with data on soil properties from Nor Yauyos Cochas (Table 4). The resulting significant Kendall's tau values can be seen in table 4. Soil organic matter is significantly correlated with elevation. Organic matter is also positively correlated with sand content and negatively correlated with clay content.

## Conclusions

Erosion and deposition values from the USPED model are mainly a function of topography for the study area. This can be seen in the distribution of values from the different model results. Distribution of values from the model using only topographic forcing closely resemble those using all USPED variables. Field data supports these results, as rangeland condition and percent cover types are all negatively correlated with slope. The ASTER DEM used for the model was successful in capturing spatial variability of slope and aspect across the study areas, as the correlation analysis between observed and measured values showed a significant meaningful relationship.

Methods used in this study for estimating percent vegetative cover were unable to capture spatial heterogeneity of vegetative cover seen in the field. Each ground control point estimated vegetative cover within a 10 meter radius, and the scale of the remotely sensed vegetative cover estimates were 30 meters by 30 meters. The discrepancies between observed and predicted percent of vegetated cover is most likely a combination of within pixel variability and human error in estimation. Temporal variability in vegetation cover may have also played a role in the inaccuracies seen, as some of the data were collected in October, which is the beginning of the rainy season, while the rest was collected in July and August, toward the end of the dry season. The satellite imagery used is from the dry season so as to minimize effects of cloud cover.

Methods for estimating soil properties were also unable to accurately reflect measured field conditions. Since soil properties have been seen to vary with cover type in semi arid rangelands, it would be expected that predicting soil properties at this scale using a dataset with a resolution of 250 meters by 250 meters would yield little meaningful relationship.

Additional research is needed to develop a more accurate method of estimating soil properties and vegetation structure at a finer scale to better account for their role in determining

rangeland condition. UAS could be used to gather high resolution aerial imagery for at risk areas to determine vegetation cover and type. This information could also be useful in predicting soil properties based on vegetation to better account for the soil erodibility factor in the calculation of sediment transport rate. More quantitative assessments of vegetation cover and rangeland condition in the field would be useful to predict rangeland condition and better understand the drivers of rangeland degradation.

External drivers of degradation such as fire, roads, and stocking rate should also be evaluated further and incorporated into the model. This may help explain areas in poor condition that are classified as stable by the model.

While vegetative cover estimates were unable to predict localized field conditions, they were useful in conducting a regional analysis of vegetative cover for the entire study area. This information is an important component in creating a land cover classification for the study area. This provides a basis to conduct a regional analysis of the susceptibility of suitable grazing areas to rangeland degradation.

Based on the results of the study, the rangeland degradation risk model appears to be more effective in the Andean puna than in the Cordillera Blanca. This was determined by comparing observed rangeland condition to the predicted condition at the ecosite scale. The larger mountains in the Cordillera Blanca resulted in a more homogenous land cover classification, as the grazing areas are much larger. This makes it much more difficult to generalize erosion rate or rangeland condition based off of ecosite. Furthermore, the bare rock and glaciers seen at higher elevations provide an additional source of water not accounted for in the calculation of erosion rate and behave differently than rangelands. This makes it more difficult to estimate erosion rates based on topography in absence of reliable soil and vegetation data. In contrast, the smaller foothills of the Andean Puna give way to a more heterogeneous landscape with smaller ecosites, making it easier to identify localized areas at risk of rangeland degradation. The two study areas are subject to different stressors, as the grazing lands in

Thomas are mainly used by llamas and alpacas, Canchayllo is mainly sheep and cattle, and Huascaran National Park is all cattle.

While the Rangeland Degradation Risk Model was unable to predict degradation at the scale of a Landsat pixel due to spatial heterogeneity, it can provide a regional analysis of degradation risk based on the topographic forcing on sediment transport. This can be used to identify grazing areas that are at risk of rangeland degradation for future monitoring and to inform management decisions in these locations. Another shortcoming of the model is that it does not account for degradation due to heavy land use in absence of accelerated erosion. Flat areas may be classified as stable due to low sediment transport rate, but may be degraded due to heavy land use. Being able to remotely sense changes in vegetative cover would allow this to be accounted for in the model.

References

Abel, N., H. Ross, and P. Walker. 1998. Mental models in rangeland research, communication, and management. The Rangeland Journal. 20(1): 77-91.

Baied, C. A. and J. C. Wheeler. 1993. Evolution of high Andean puna ecosystems: environment, climate, and culture changeover the last 12,000 years in the Central Andes. Mountain Research and Development 13:145 156.

Byers, A. C. 2000. Contemporary landscape change in the Huascaran National Park and buffer zone, Cordillera Blanca, Peru. Mountain Research and Development 20:52-64.

Drenkhan, F., M. Carey, C. Huggel, J. Seidel and M.T. Ore. 2015. The changing water cycle: climatic and socioeconomic drivers of water-related changes in the Andes of Peru. WIREs Water 2:715-733.

Durigon, V.L., D. F. Carvalho, M.A.H Antunes, P.T.S. Oliveira and M.M. Fernandes. 2014. NDVI time series for monitoring RUSLE cover management factor in a tropical watershed. International Journal of Remote Sensing, 35(2): 441-453.

Eswaran, H., R. Lal and P.F. Reich. 2001. Land degradation: an overview. Responses to Land Degradation. Enfield, NH : Science Publishers. 20-35.

Feeley, K.J. and M.R. Silman. 2010. Land-use and climate change effects on population size and extinction risk of Andean plants. Global change biology, 16(12): 3215-3222.

Fonken, M. 2014. An introduction to the bofedales of the Peruvian High Andes. Mires & Peat 15:1-13.

Gallacher, D. 2015. Ecological Monitoring of Arid Rangelands using Micro-UAVs (drones). Sixth Health and Environment Conference, HBMsU Congress, At Dubai, UAE

Gutman, G. & A. Ignatov. 1998. The derivation of the green vegetation fraction from NOAA/AVHRR data for use in numerical weather prediction models, International Journal of Remote Sensing, 19(8): 1533-1543

Hengl T., J. Mendes de Jesus, G.B.M. Heuvelink, M. Ruiperez Gonzalez, M. Kilibarda. 2017. SoilGrids250m: Global gridded soil information based on machine learning. PLOS ONE 12(2): e0169748. https://doi.org/10.1371/journal.pone.0169748

Krausman, P.R., D.E. Naugle, M.R. Frisina, R. Northrup, V.C. Bleich, W.M. Block, M.C. Wallace, and J.D. Wright. 2009. Livestock grazing, wildlife habitat, and rangeland values. Rangelands, 31(5), 15-19.

Kumar, R. and A.J. Das. 2014. Climate change and its impacts on land degradation: imperative need to focus. Journal of Climatology and Weather Forecasting, 2(1): 2332-2594.

Mitasova, H., J. Hofierka, M. Zlocha, and L.R. Iverson. 1996. Modelling topographic potential for erosion and deposition using GIS. International Journal of Geographical Information Systems, 10(5): 629-641.

Lozada, C. 1991. Overgrazing and range degradation in the Peruvian Andes. Rangelands 13(2): 64-67.

Millones, J. 1982. Patterns of land use and associated environmental problems of the Central Andes: An integrated summary. Mountain Research and Development 2:49-61.

Milton, S.J., M.A. du Plessis, and W.R. Siegfried. 1994. A conceptual model of arid rangeland degradation. Bioscience, 44(2): 70-76.

Oficina Nacional de Evaluacion de Recursos Naturales (ONERN). 1976. Mapa Ecologico Del Peru: Guia Explitiva, ONERN, http://repositorio.ana.gob.pe/handle/ANA/1052. Accessed May 2018.

Shoobridge, D. 2005. Huascaran National Park. ParksWatch Peru. https://www.parkswatch.org/parkprofile.php?l=eng&country=per&park=hunp. Accessed October 2017.

Pizarro, S. 2017. Degradación y vulnerabilidad al cambio climático en pastizales altoandinos, Universidad Nacional Agraria La Molina. Escuela de Posgrado. Maestría en Producción Animal. http://repositorio.lamolina.edu.pe/handle/UNALM/2916

Pricope, N. 2009. Assessment of Spatial Patterns of Sediment Transport and Delivery for Soil and Water Conservation Programs, Journal of Spatial Hydrology 9(1): 21-46

Renard, K., G. R. Foster, G. A. Weesies, and J.P. Porter. 1991. RUSLE: Revised Universal Soil Loss Equation. Journal of Soil and Water Conservation, 46(1): 30-33.

Renard, K.G. and J.R. Freimund. 1994. Using monthly precipitation data to estimate the R-factor in the revised USLE. Journal of Hydrology. 157:287-306.

Servicio Nacional de Áreas Naturales Protegidas por el Estado (SERNANP). 2012. Huascarán: Servicio Nacional de Áreas Naturales Protegidas por el Estado. Lima,Peru: Author

Servicio Nacional de Áreas Naturales Protegidas por el Estado (SERNANP). 2016. Reserva Paisajistica Nor Yauyos Cochas Plan Maestro 2016-2020. Lima, Peru: Author

Society for Range Management. 2019. Policy Statements. https://rangelands.org/about/policy-statements/. Accessed March 2019.

Stavi, I., E. Ungar, H. Lavee, and P. Sarah. 2008. Grazing-induced spatial variability of soil bulk density and content of moisture, organic carbon and calcium carbonate in a semi-arid rangeland. Catena., 75(3): 288-296.

Tachikawa, T., M. Hato, M. Kaku, and A. Iwasaki. 2011. Characteristics of ASTER GDEM version 2. In 2011 IEEE international geoscience and remote sensing symposium (3657-3660). IEEE.

Universidad Nacional Agraria La Molina Laboratorio de Ecologica y Utilizacion de Pastizales. 2016.

Warren, S. D., H. Minasova, M. G. Hohmann, S. Landsberger, F. Y. Iskander, T. S. Ruzycki, and G. M. Senseman. 2005. Validation of a 3-D enhancement of the Universal Soil Loss Equation for prediction of soil erosion and sediment deposition. Catena 64:281-296

Westoby, M., Walker, B., & Noy-Meir, I. 1989. Opportunistic management for rangelands not at equilibrium. Journal of range management, 42(4): 266-274.

Wischmeier, W.H. and D.D. Smith. 1978. Predicting rainfall erosion losses-a guide to conservation planning. Predicting rainfall erosion losses-a guide to conservation planning.

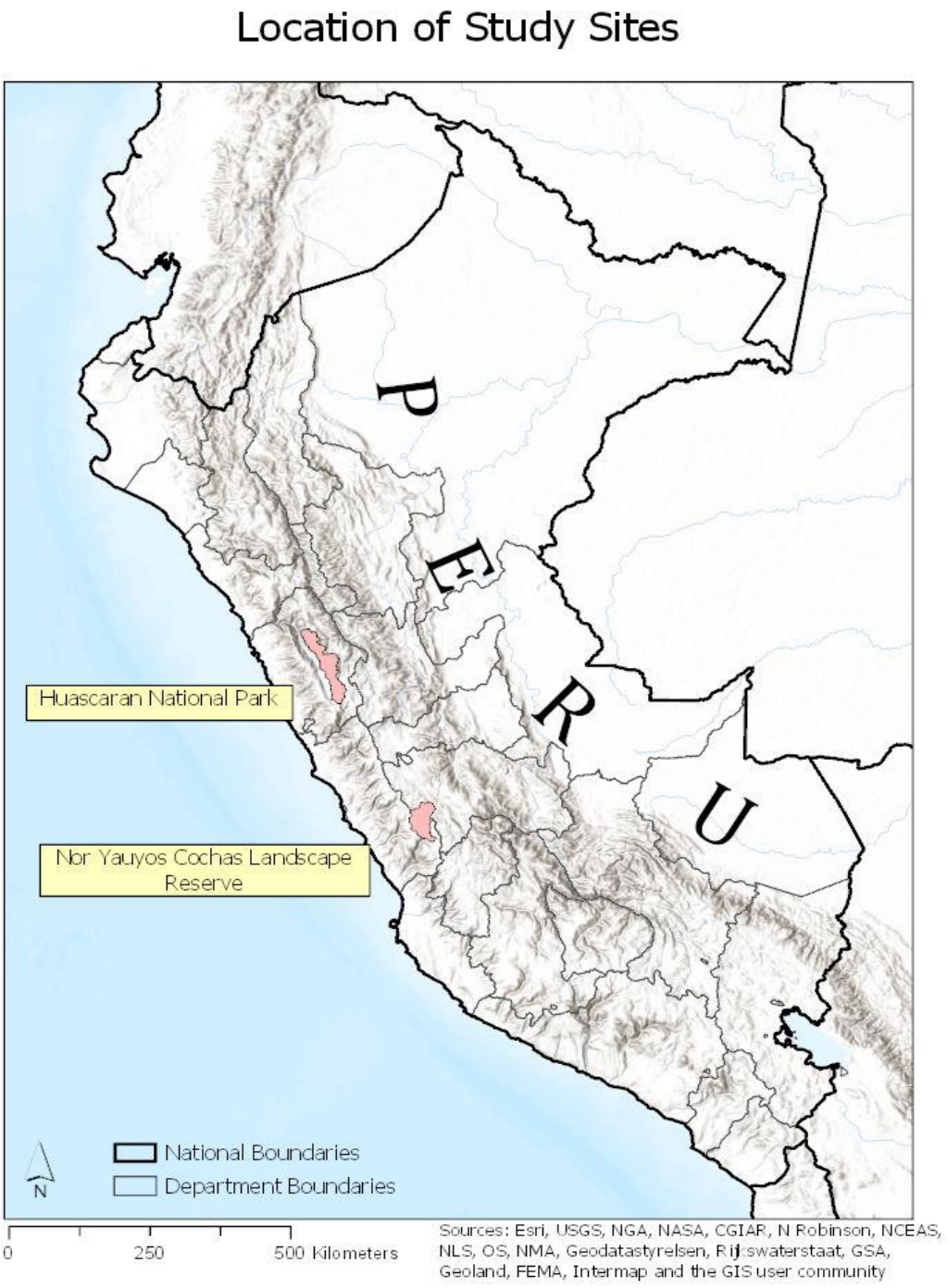


Figure 1: Location of study areas in Peru.

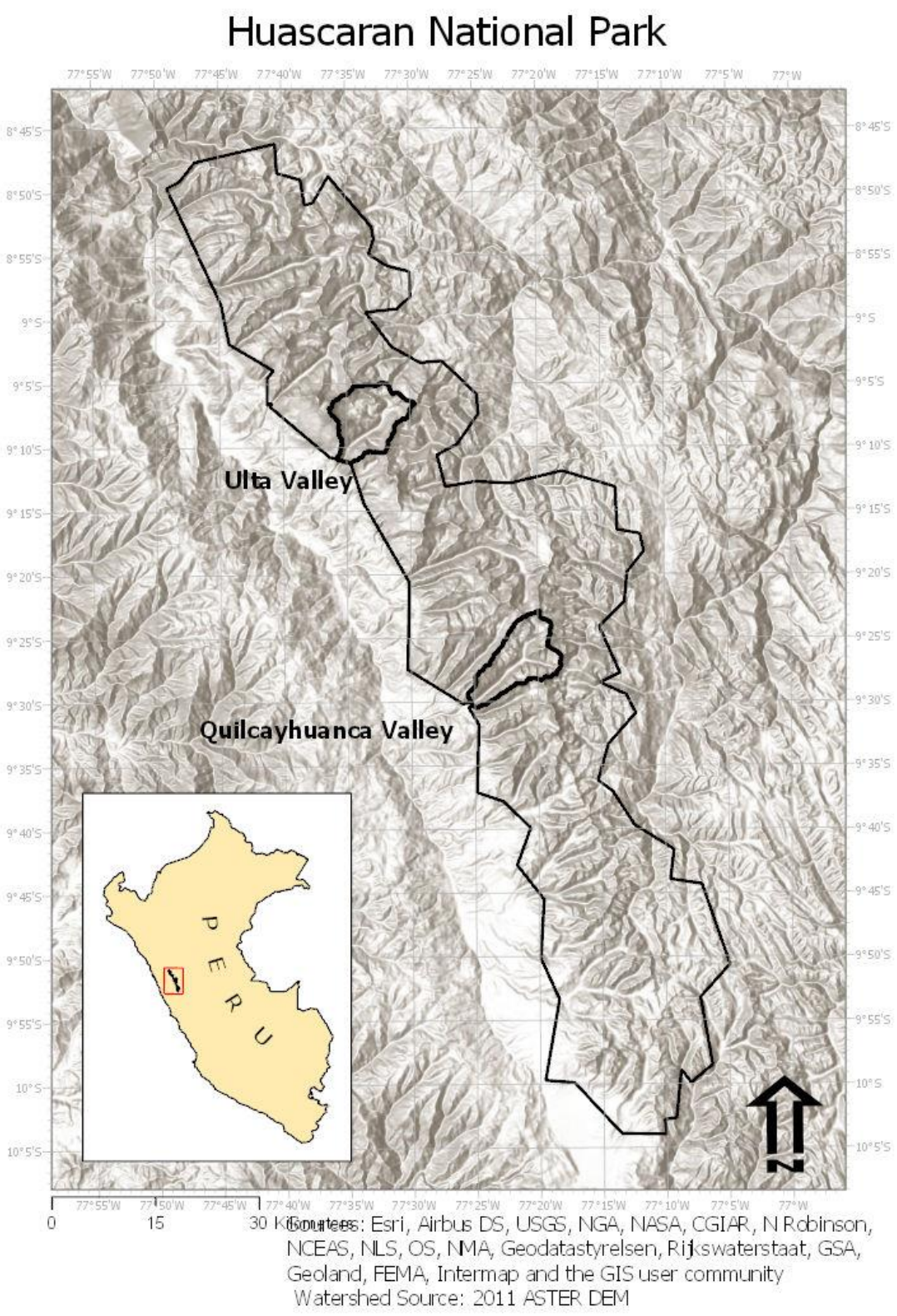


Figure 2: Ulta and Quilcayhuanca Valleys in Huascaran National Park

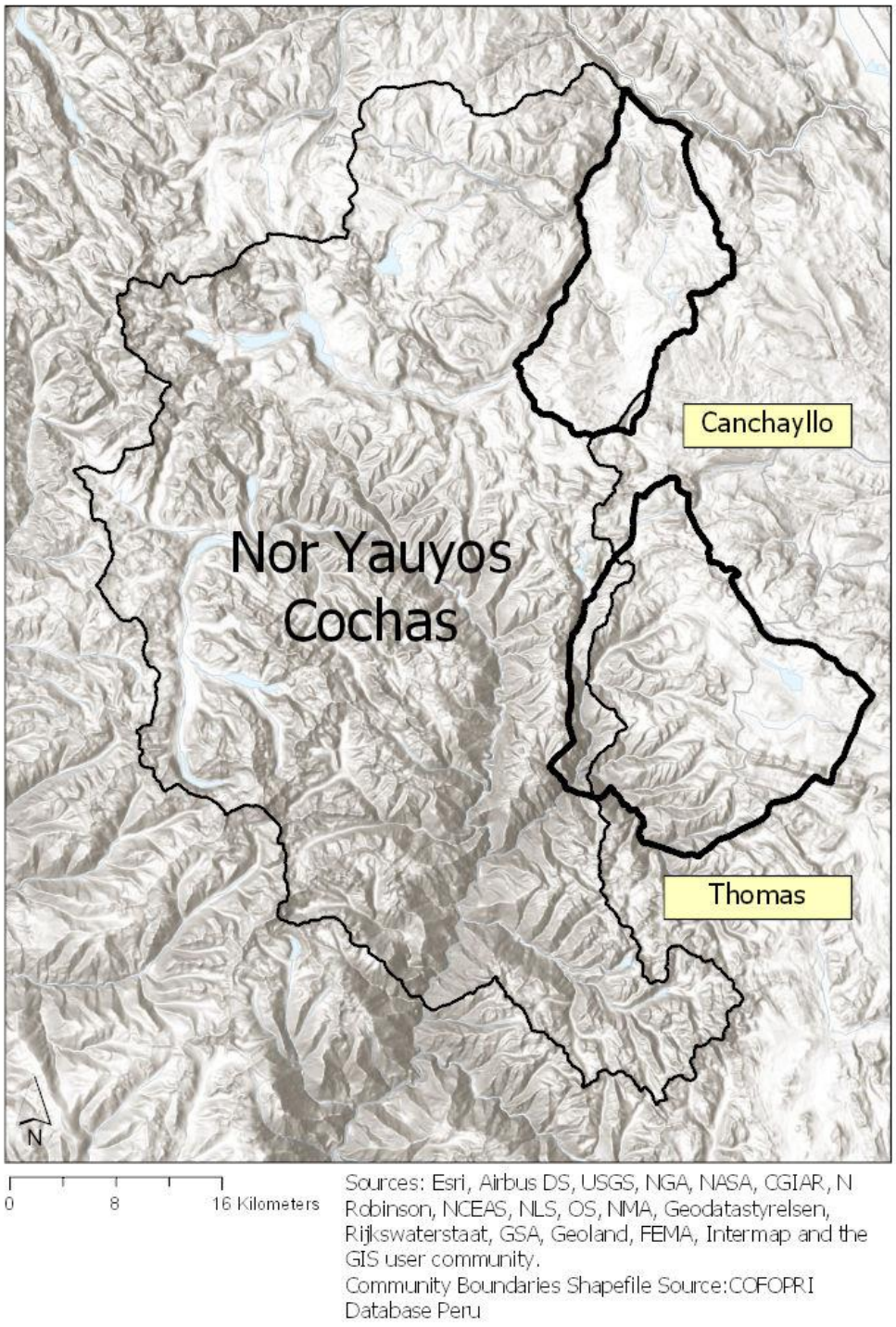


Figure 3: Canchayllo and Thomas communities within Nor Yauyos Cochas Landscape Reserve

Table 1: Data sources and resolution for model inputs.

| **Data Inputs for USPED Model** | | | |
|---|---|---|---|
| **Data Parameter** | **Source** | **Resolution** | **Period** |
| Slope, Aspect, and Elevation | ASTER DEM | 30 Meters | 2011 |
| Vegetative cover | Landsat | 30 Meters | November to April 2014 - 2018 |
| Vegetative cover | Moderate Resolution Imaging Spectroradiometer (MODIS) | 250 Meters | 2015-2018 |
| Rainfall | Climate Hazards Group InfraRed Precipitation with Station data (CHIRPS) | 0.05 decimal degrees | Monthly 1981-2018 |
| Surface percentage of sand, silt, and clay | SoilGrids | 250 Meter | 2017 |

Table 2: Data sources used to create supervised land cover classification

| **Data Inputs for supervised Land Cover Classification** | |
|---|---|
| **Data** | **Source** |
| Elevation | 2011 ASTER DEM (Tachikawa et al. 2011) |
| Humidity Regime | ONERN 1976 |
| Land Cover | July 2017 Landsat 8 Imagery obtained from the U.S. Geographical Survey |
| Regions of Interest | Universidad Nacional Agraria La Molina Laboratorio de Ecología y Utilización de Pastizales 2016 |

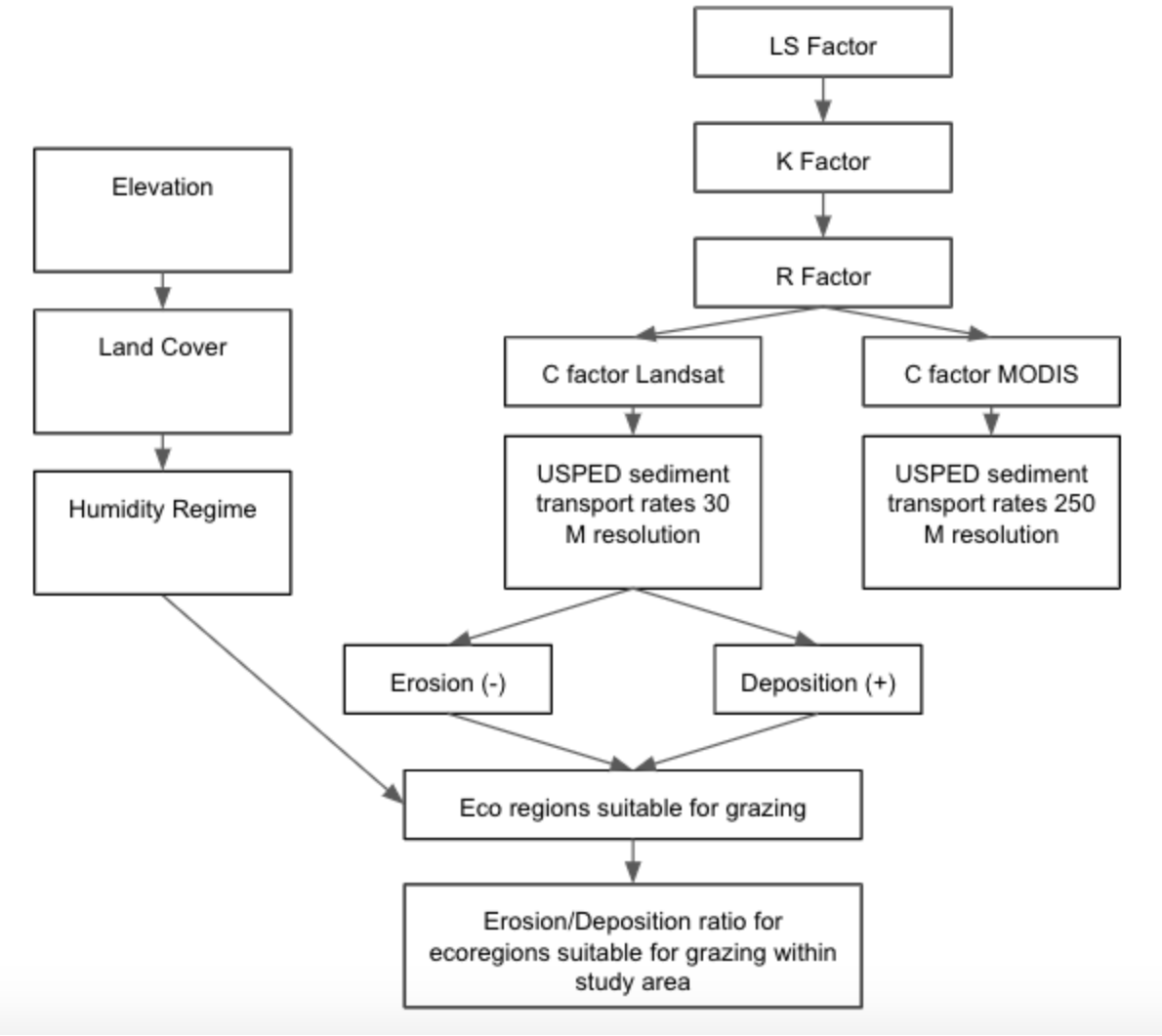


Figure 4: Flowchart detailing process of development of Rangeland Degradation Risk Model

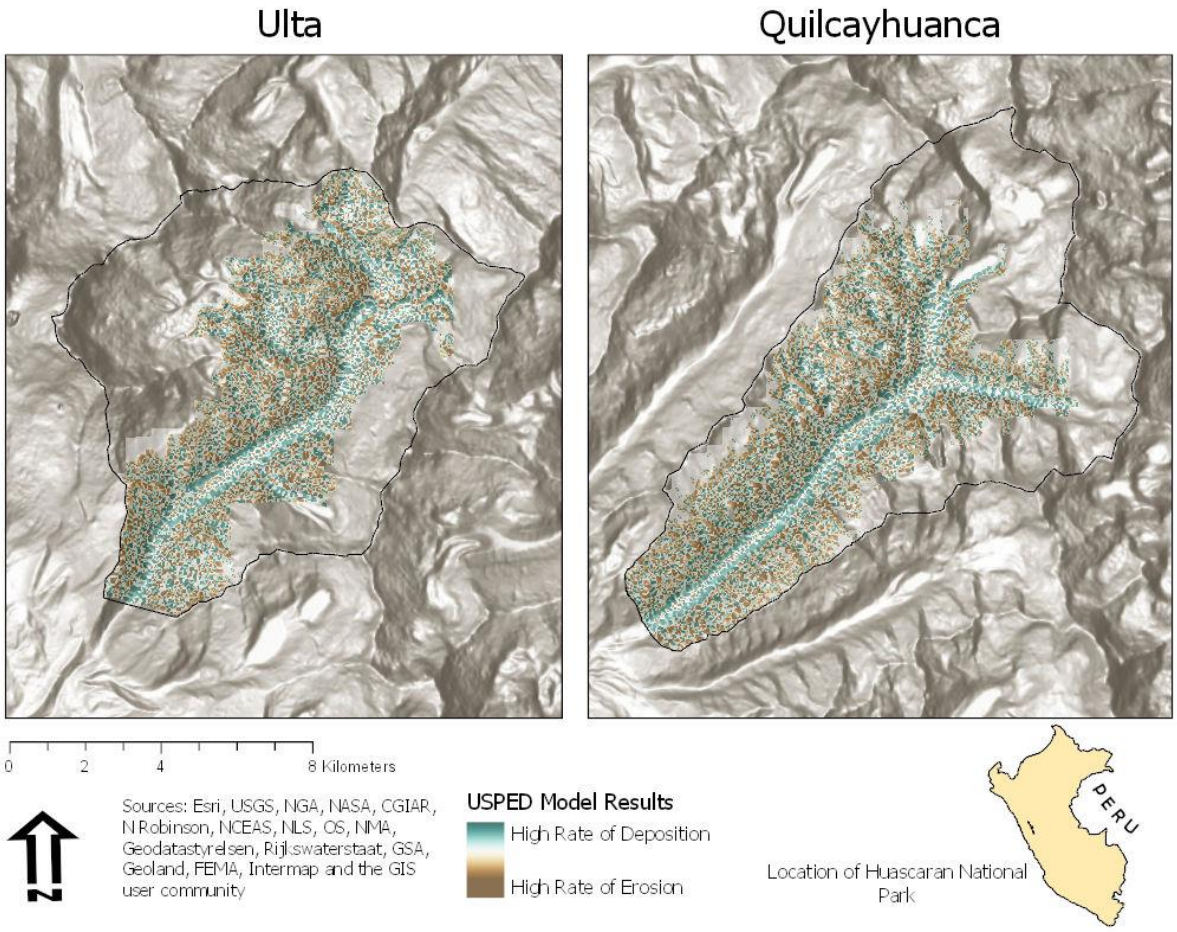


Figure 5: Results of USPED model at the Landsat pixel scale for Huascaran National Park

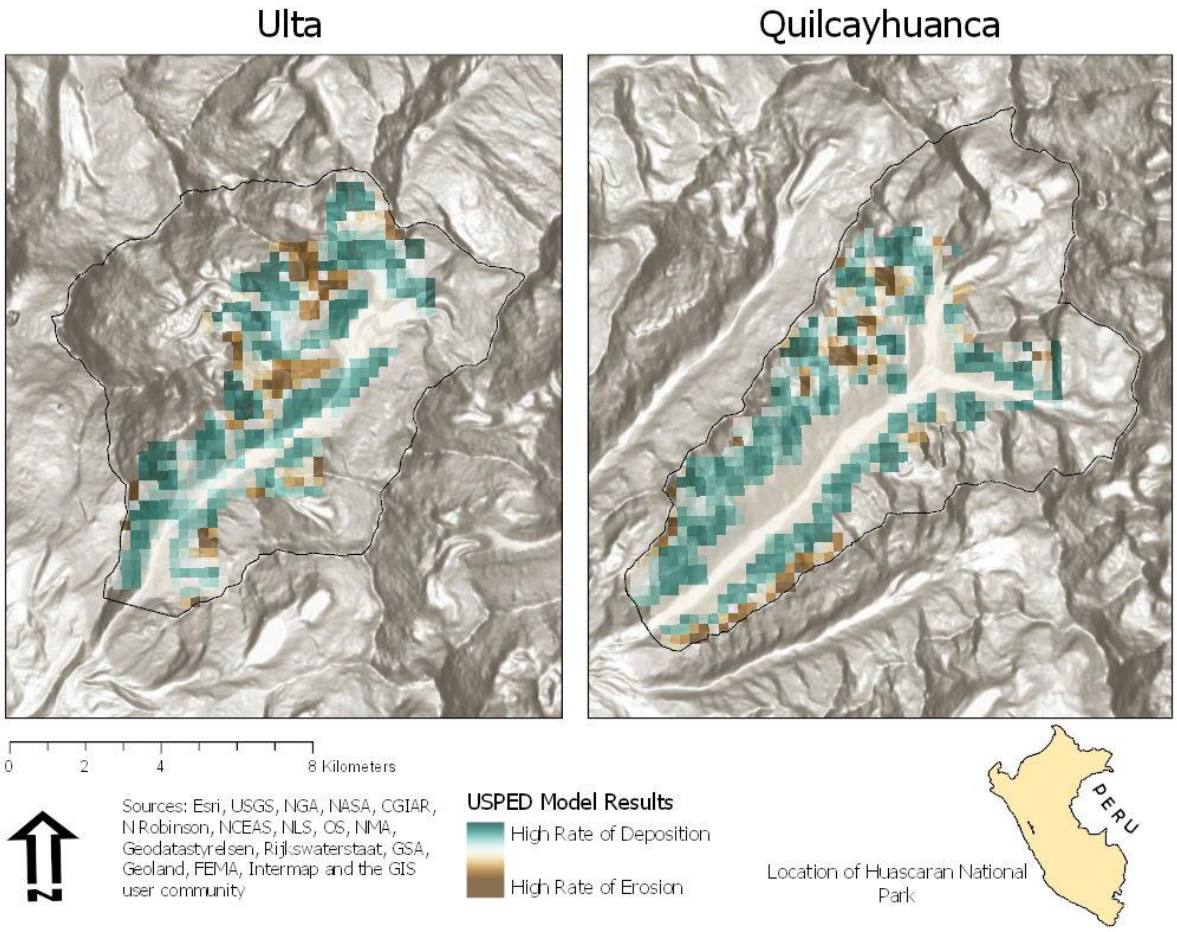


Figure 6: Results of USPED model at the MODIS pixel scale for Huascaran National Park

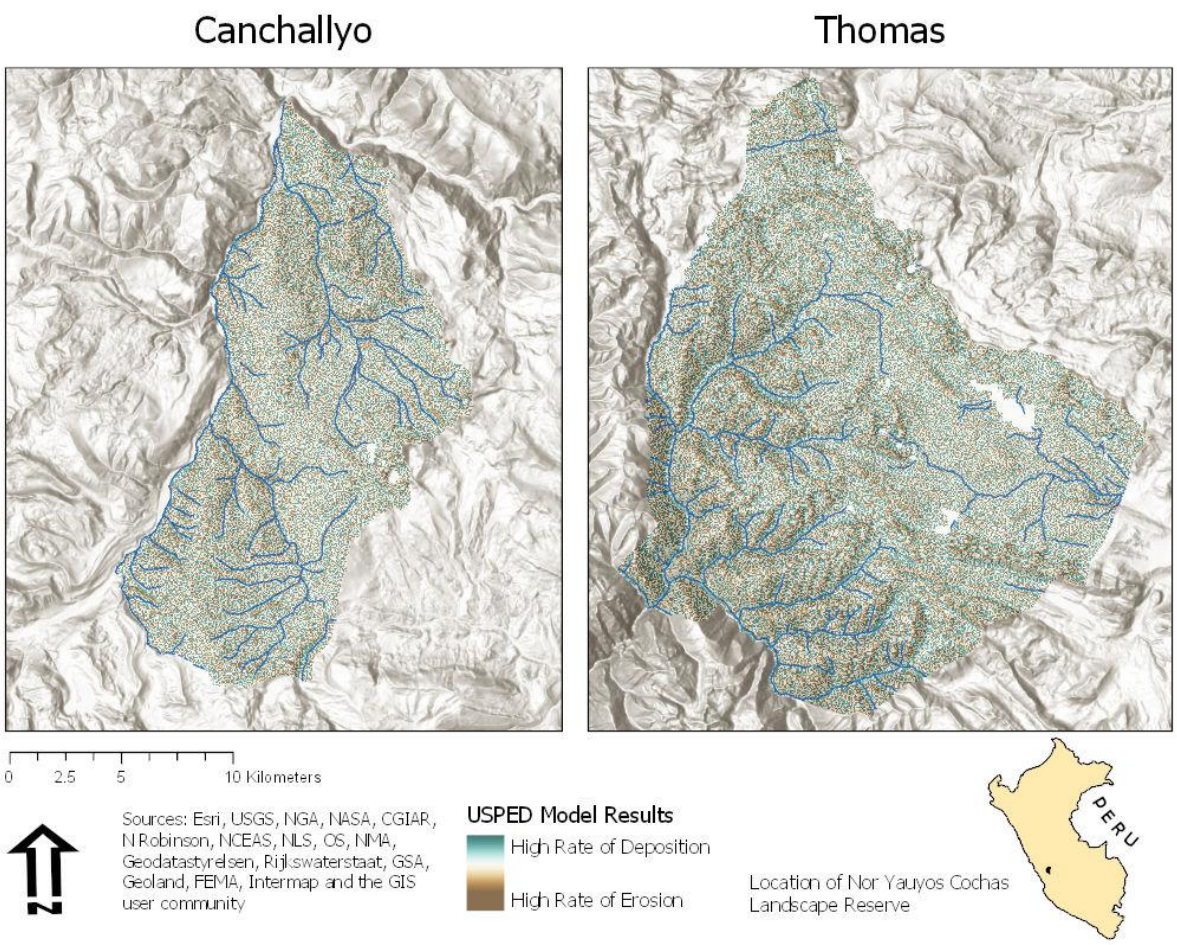


Figure 7: Results of USPED model at the Landsat pixel scale for Nor Yauyos Cochas

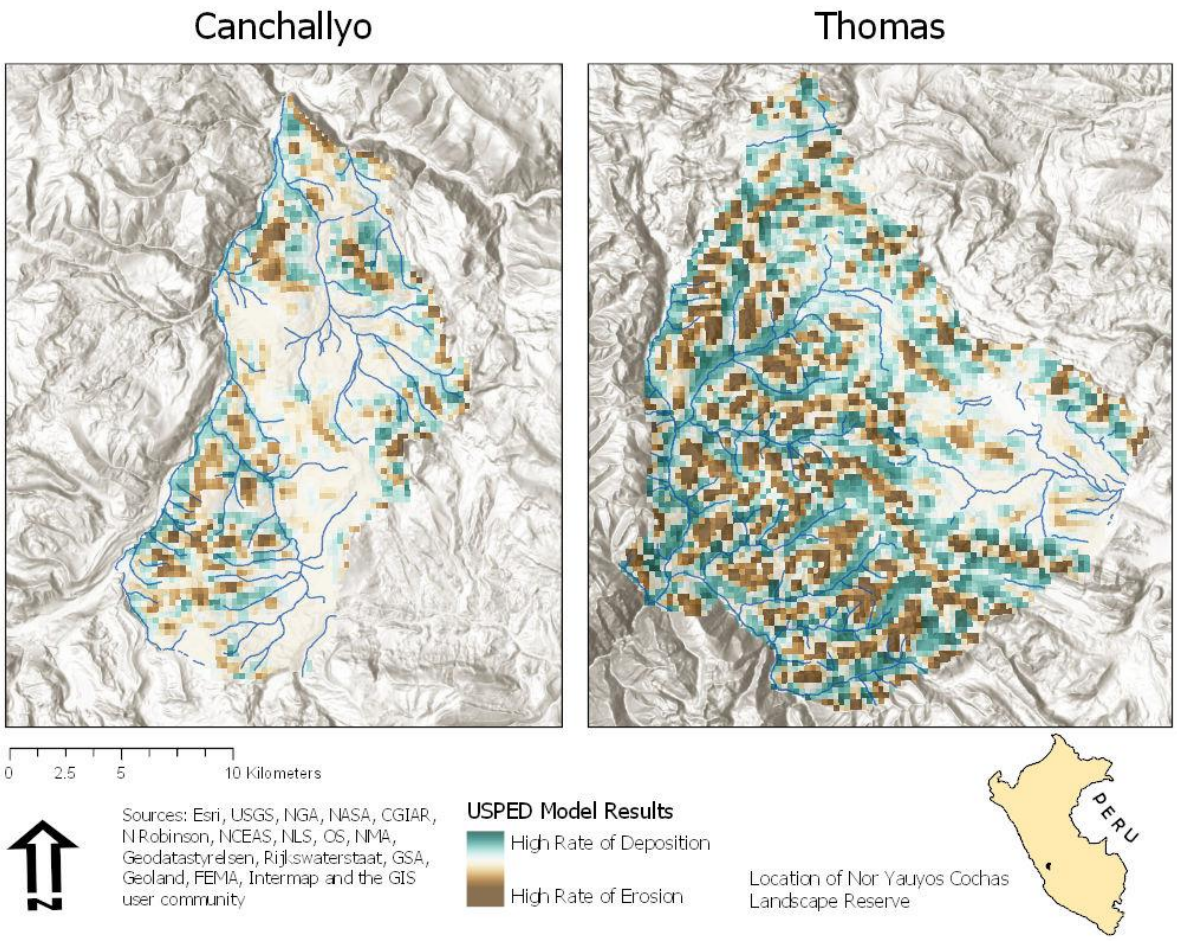


Figure 8: Results of USPED model at the MODIS pixel scale for Nor Yauyos Cochas

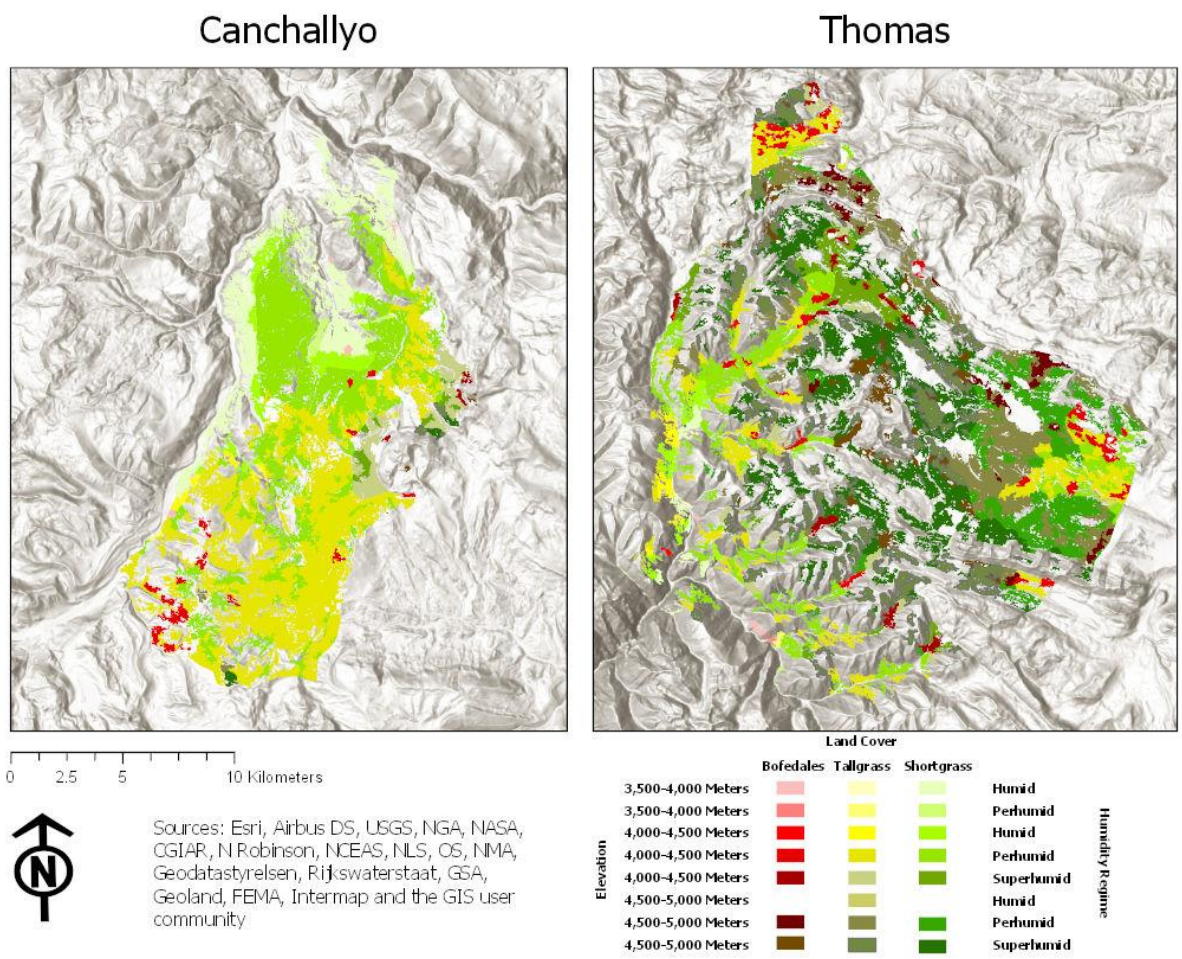


Figure 9: Supervised land cover classification for suitable grazing areas in Thomas and Canchayllo communities in Nor Yauyos Cochas Landscape Reserve.

Figure 10: Example of tallgrass ecosystem in Canchayllo.  Looking north from GCP 112 toward a large shortgrass area.  Gentle, undulating topography results in uninterrupted

Figure 11: Shortgrass and tallgrass ecosites in Thomas.  Photo taken from GCP 130.  Steep slopes and rocky outcrops segment areas suitable for grazing

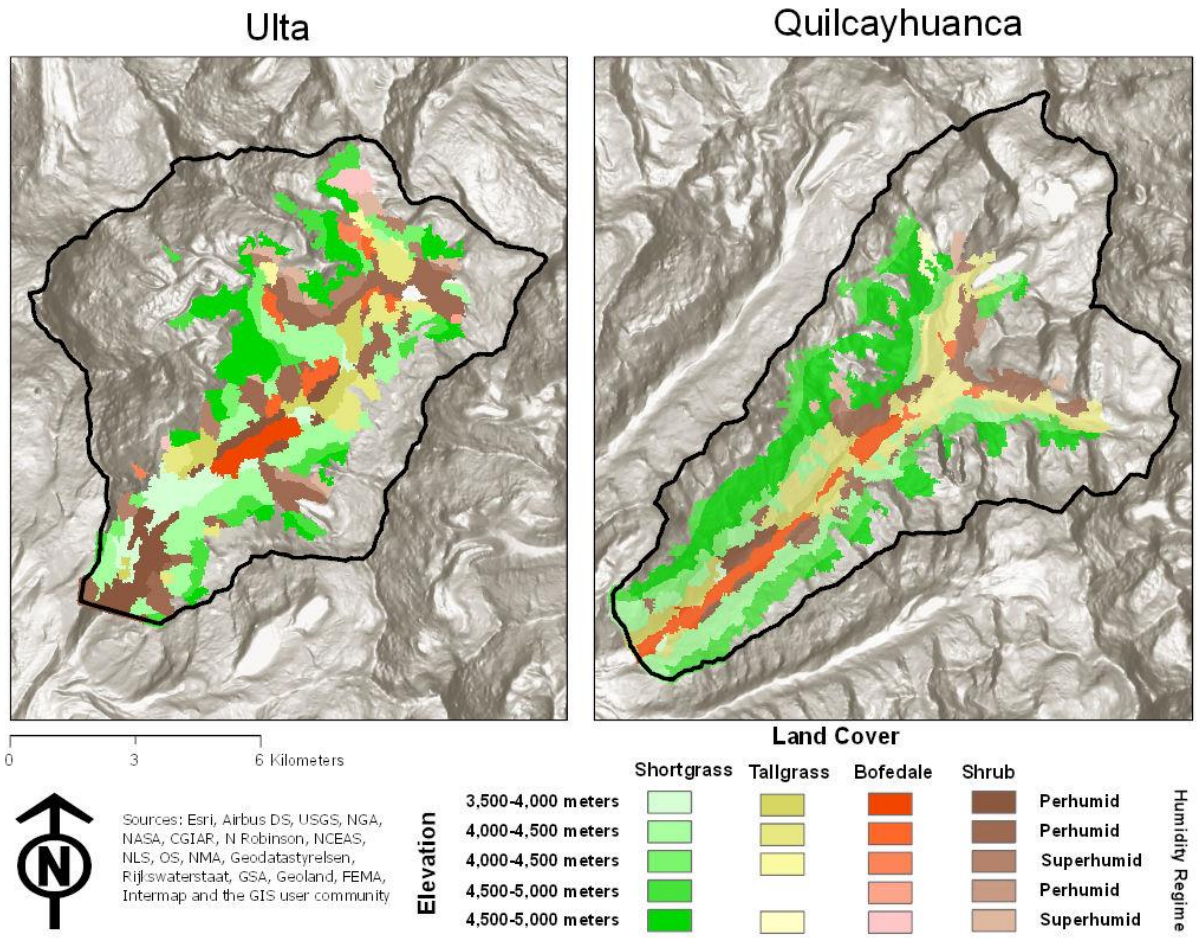


Figure 12: Supervised land cover classification for Ulta and Quilcayhuanca valleys in Huascaran National Park.

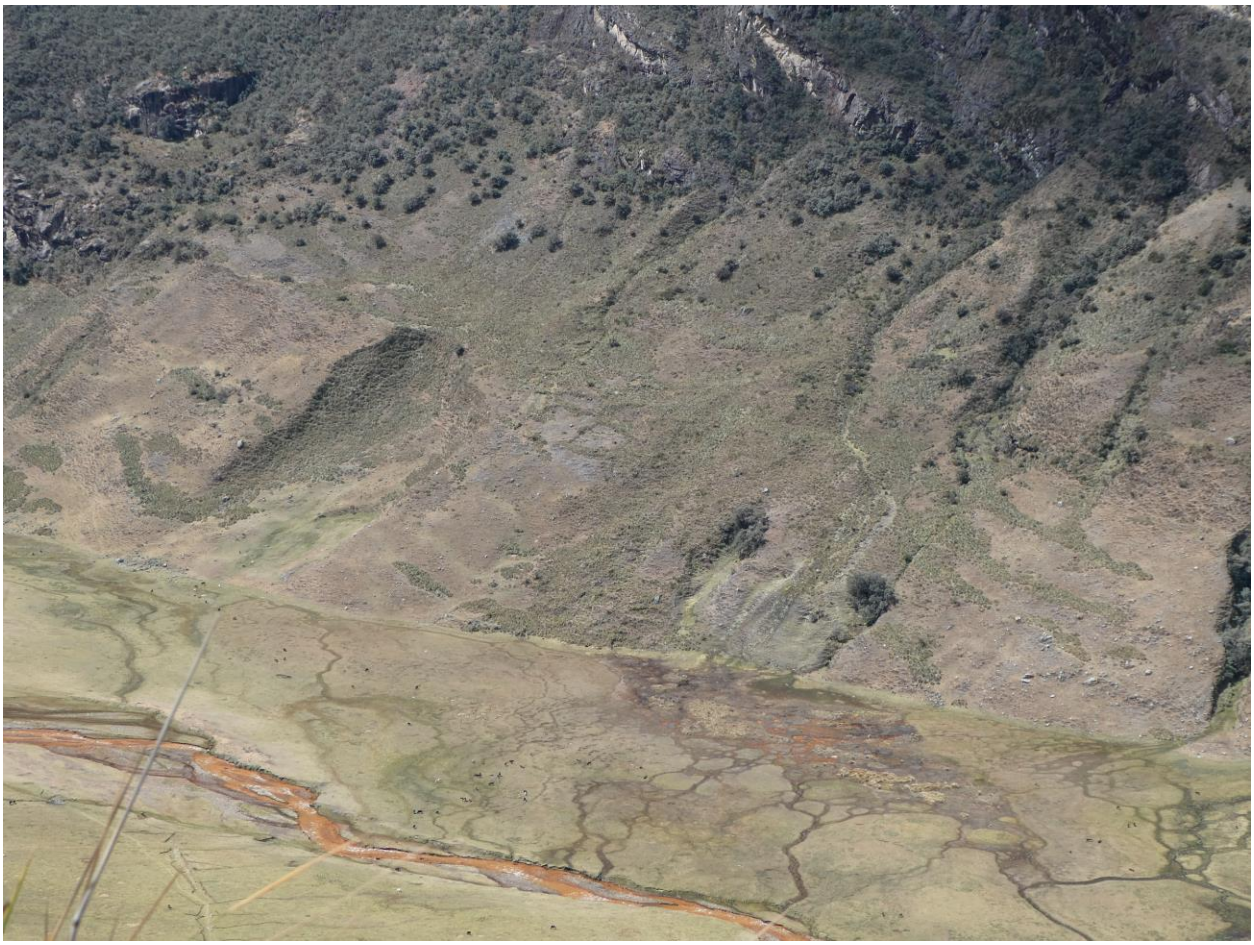

Figure 13: Visual example of how land cover and species composition changes with elevation. Photo taken from northern slope of Quilcayhuanca valley.

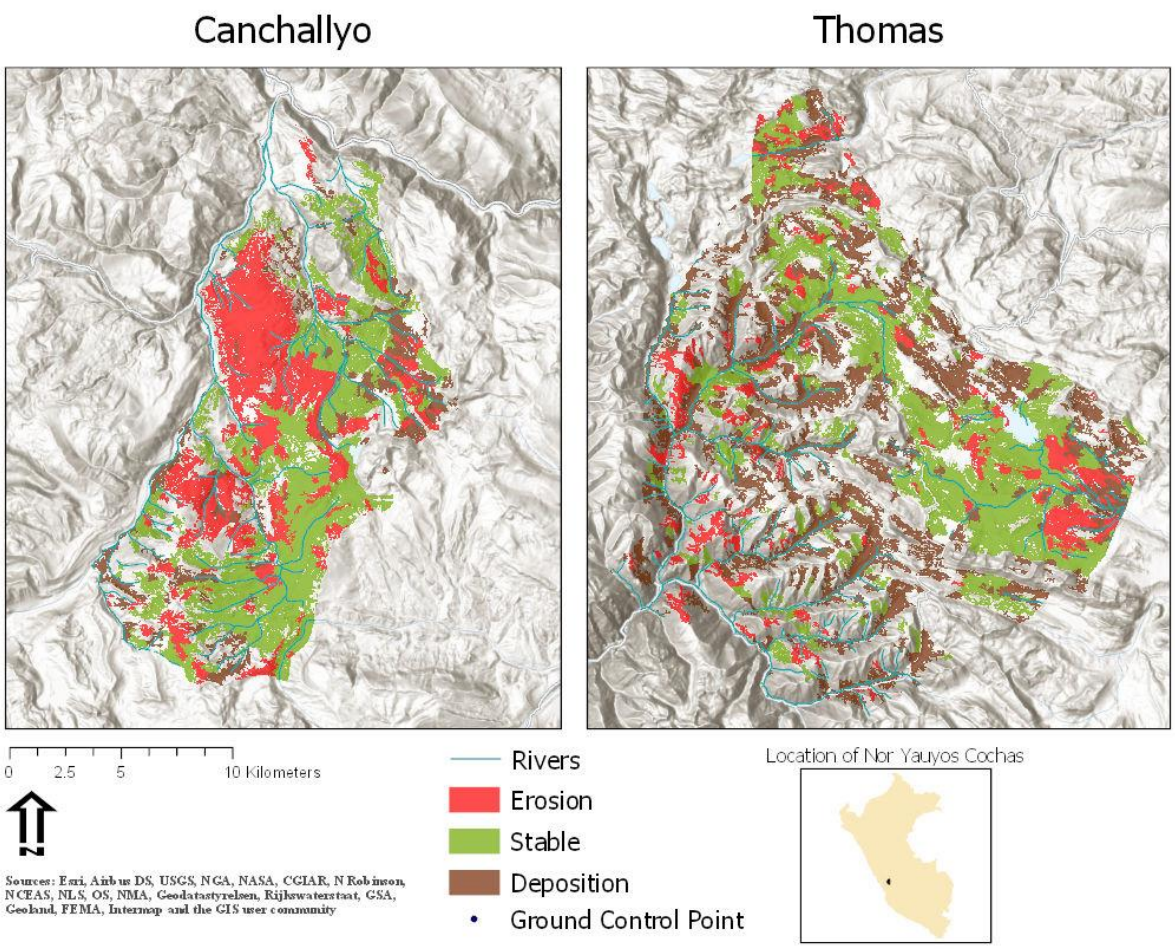


Figure 14: Erosion deposition rate calculated by ecosite for Nor Yauyos Cochas

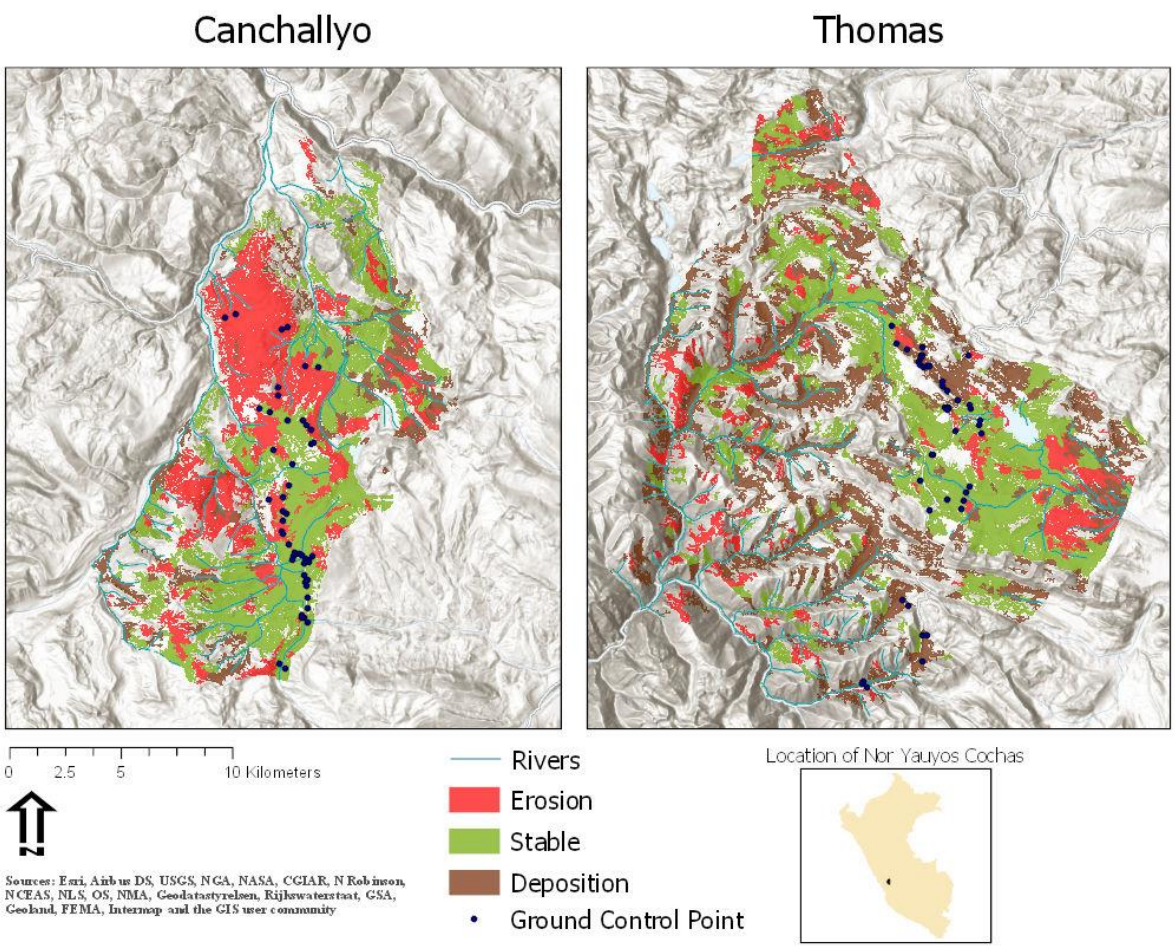


Figure 15: Erosion deposition rate calculated by ecosite for Nor Yauyos Cochas with location of ground control points.

Table 3: Confusion matrix of observed rangeland condition and predicted ecosite condition for all ground control points.

| | | Predicted Ecosite Condition | | | | | |
|---|---|---|---|---|---|---|---|
| | | Erosion | Stable | Deposition | NA | Total | **Percent Total** |
| Observed Rangeland Condition | Very Poor | 15 | 0 | 1 | 2 | **18** | **11.7%** |
| | Poor | 23 | 27 | 13 | 5 | **68** | **44.2%** |
| | Regular | 9 | 22 | 7 | 6 | **44** | **28.6%** |
| | Good | 5 | 7 | 2 | 0 | **14** | **9.1%** |
| | Excellent | 2 | 6 | 2 | 0 | **10** | **6.5%** |
| | Total | **54** | **62** | **25** | **13** | **154** | |
| | **Percent Total** | **35.1%** | **40.3%** | **16.2%** | **8.4%** | | **100%** |

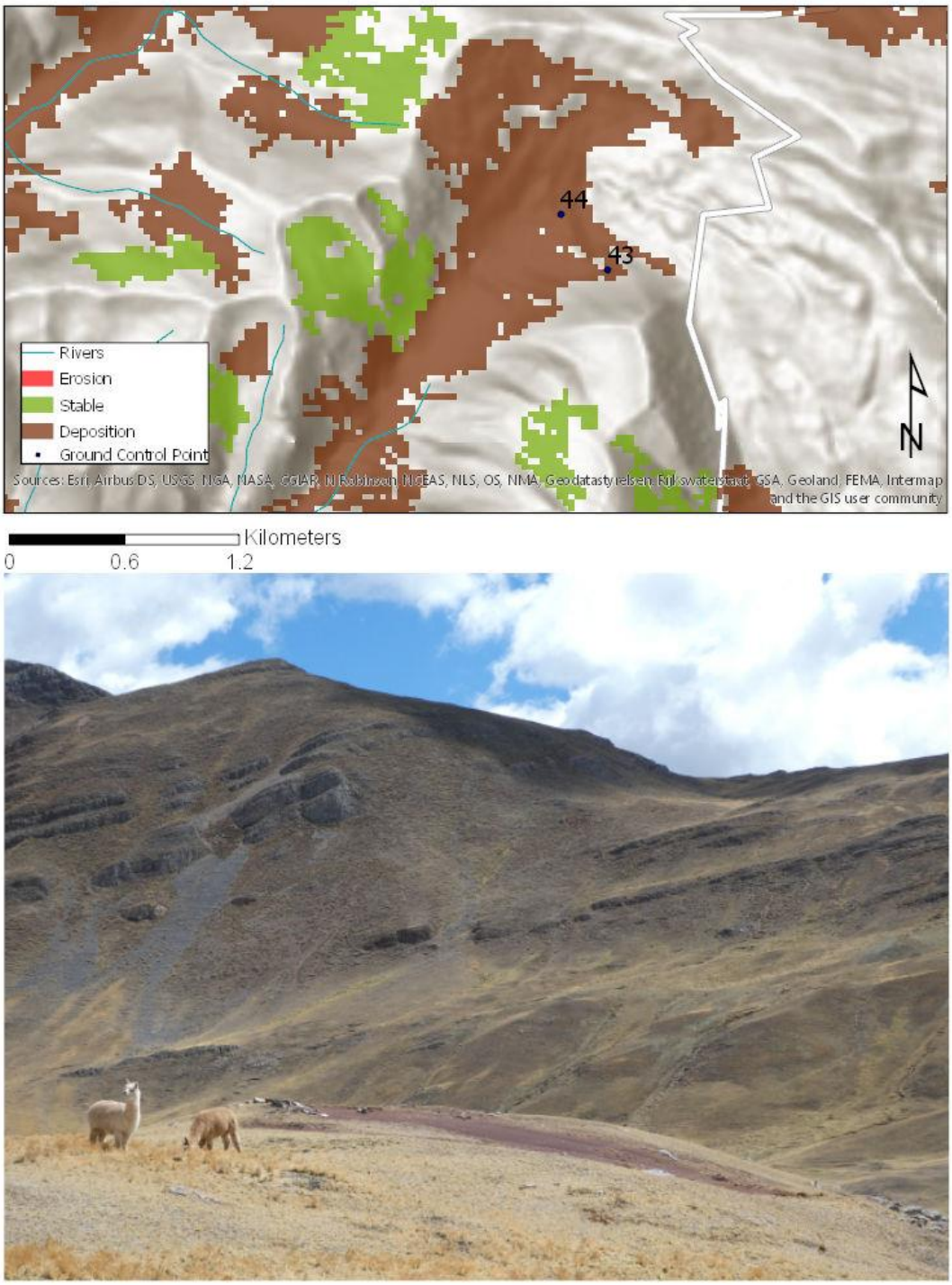


Figure 16: Predicted ecosite conditions for southeast portion of Thomas and photograph of rangelands, taken from point 44.

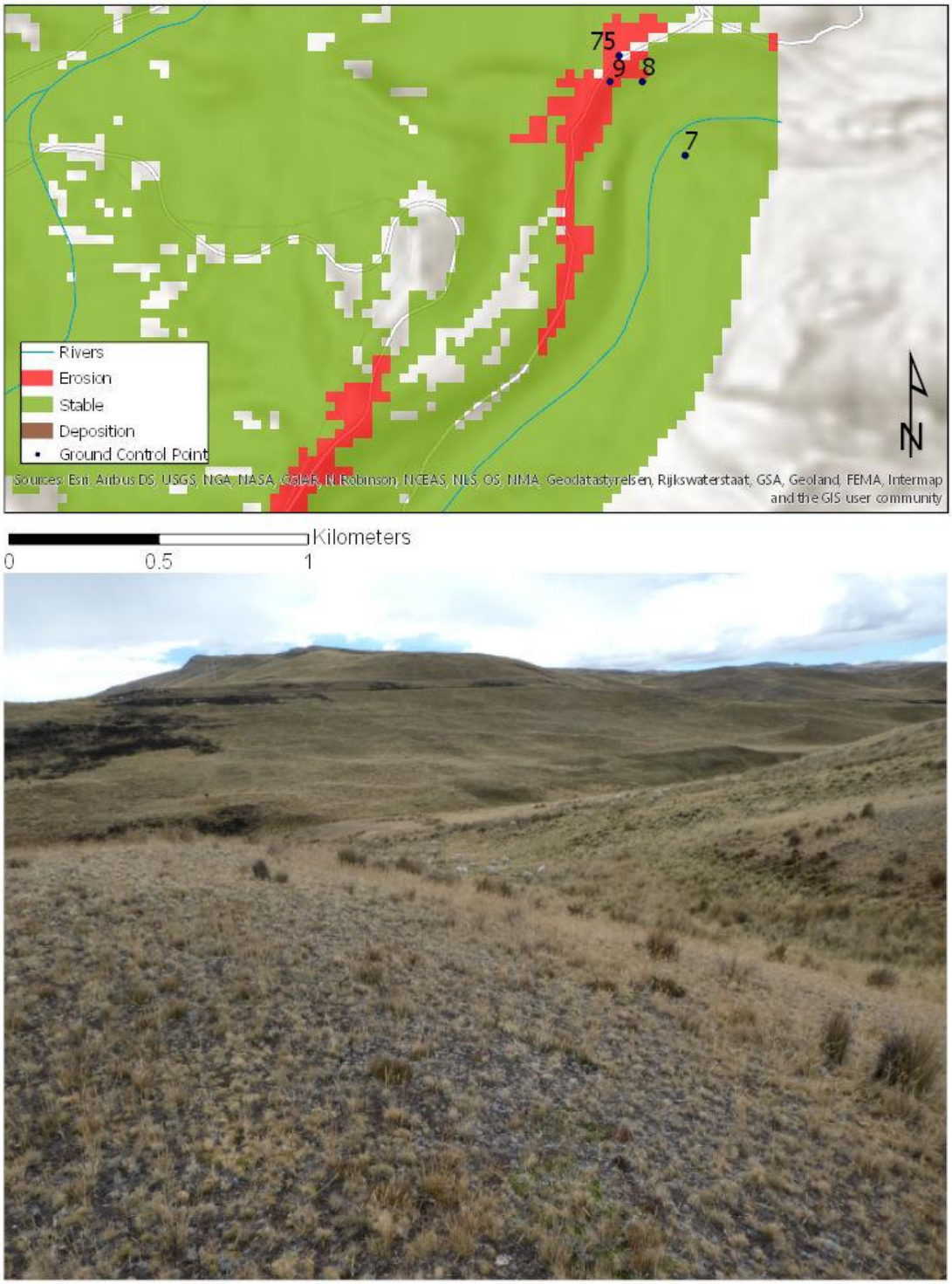


Figure 17: Predicted ecosite conditions for southeast portion of Canchayllo and photograph of rangeland, taken from point 7.

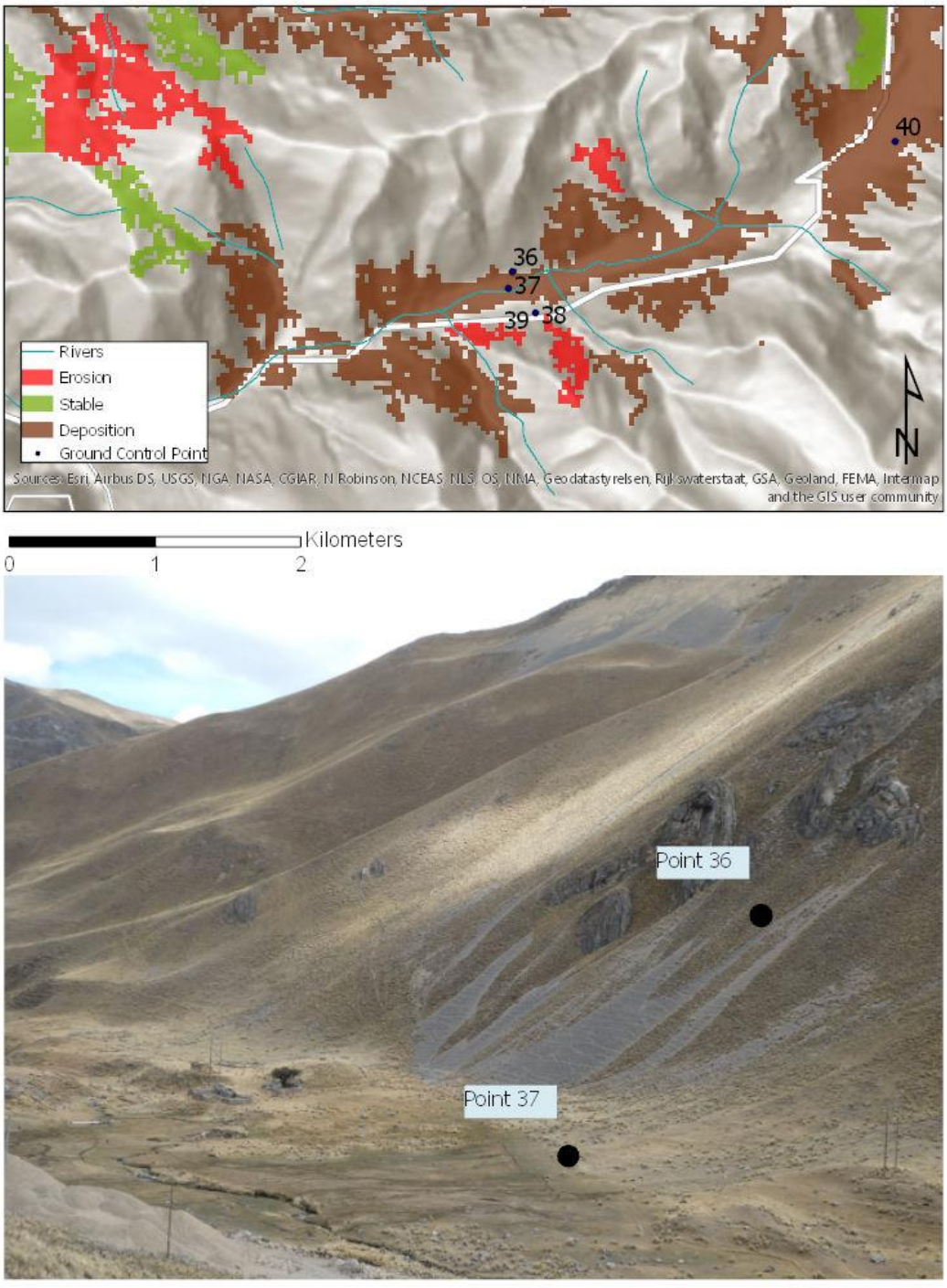


Figure 18: Eroding hillside catalyzed by heavy grazing. Footpaths for grazing animals can be seen in bare rock section. Differences in type and amount of vegetation can be seen between the two points.

Figure 19: Soil samples from point 36 (left) and point 37 (right).

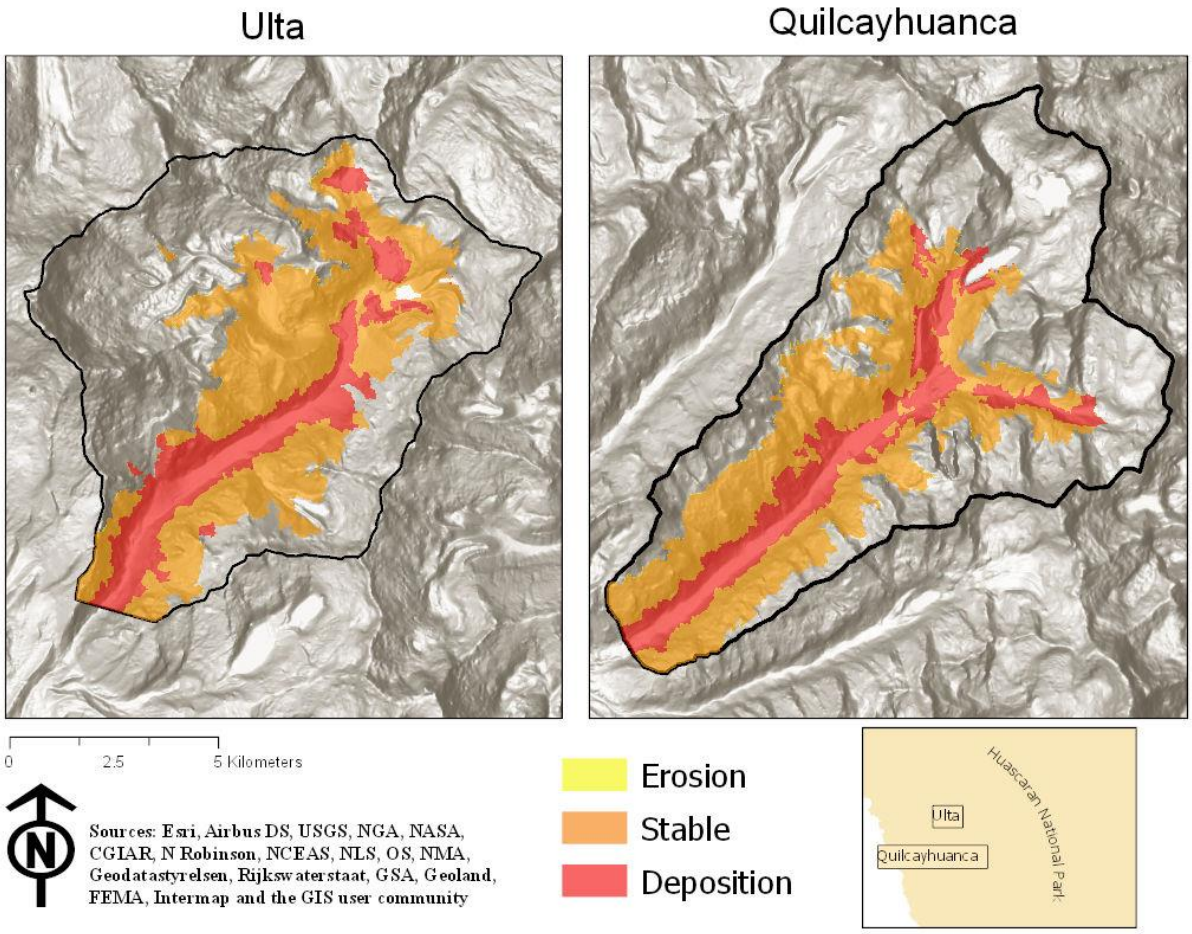


Figure 20: Erosion to deposition ratio calculated for each ecosite in Ulta and Quilcayhuanca valleys

Figure 21: Image looking northwest from the southeastern slope of Ulta Valley. Glaciers and bare rock are visible above visibly eroding hillsides in the far valley.

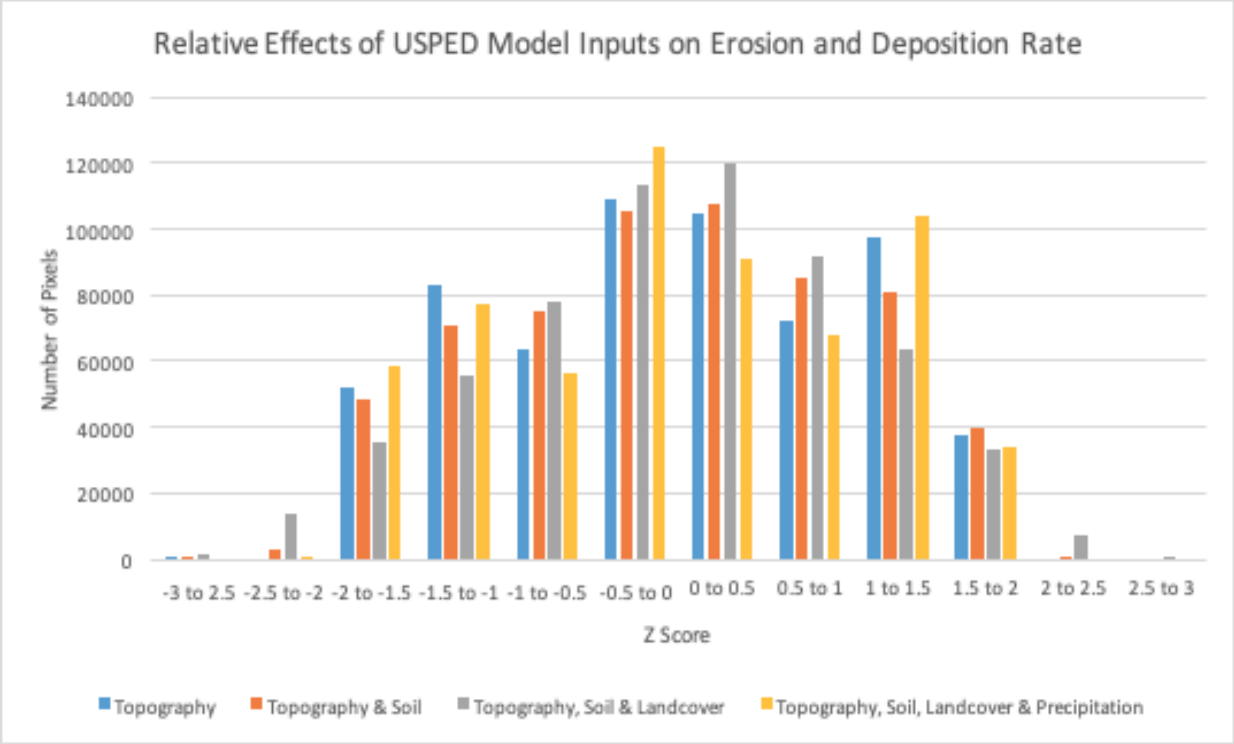


Figure 22: Histogram showing distribution of standardized values for erosion and deposition rates as a function of different variables.

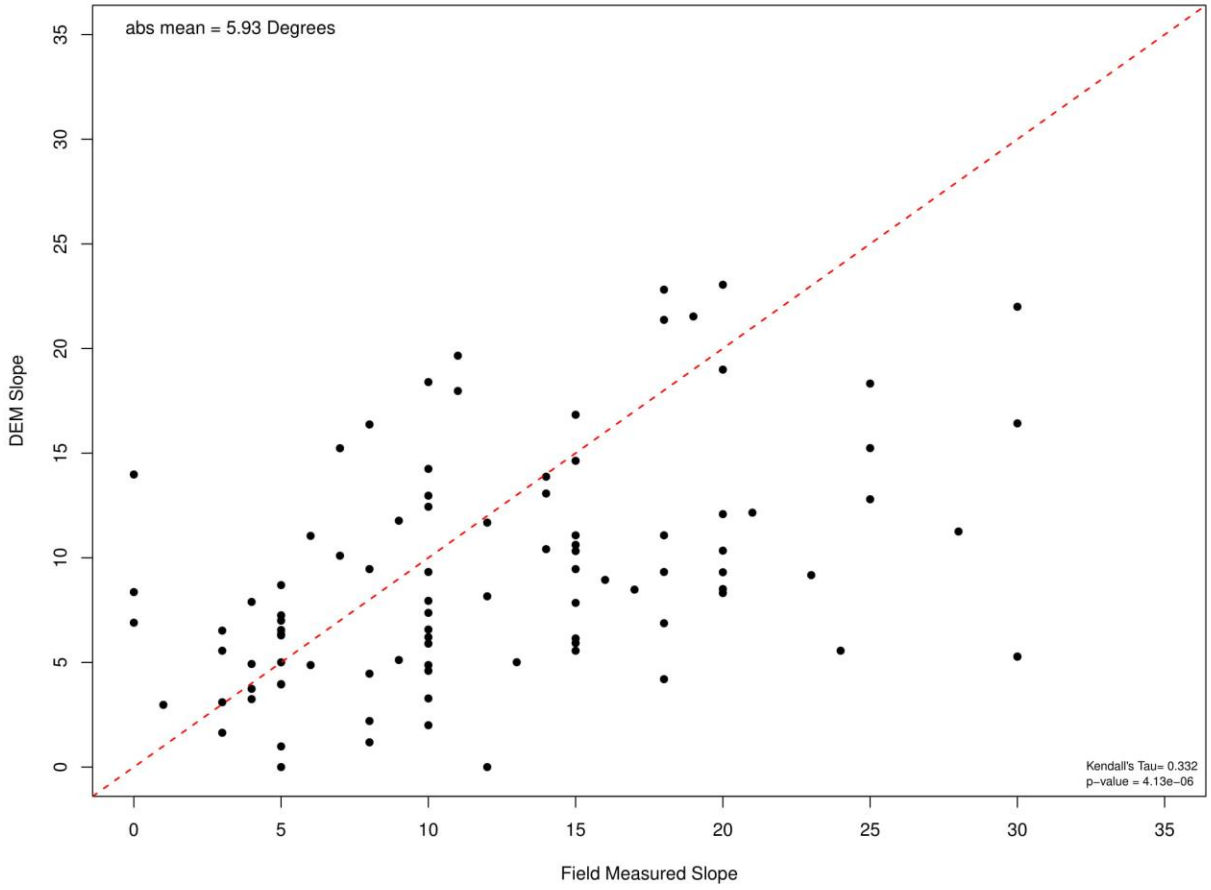


Figure 23: Measured slope compared to slope derived from DEM.

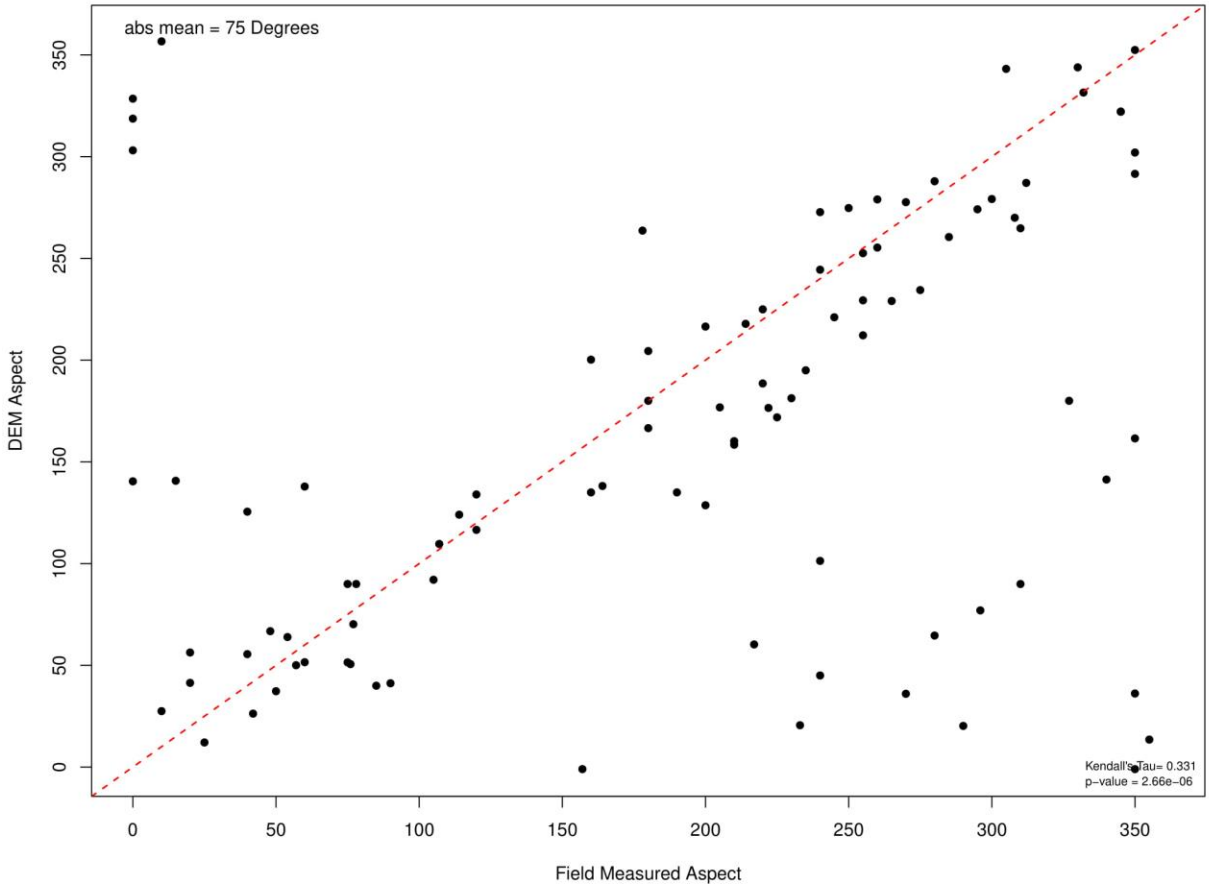


Figure 24: Measured aspect compared to aspect derived from DEM

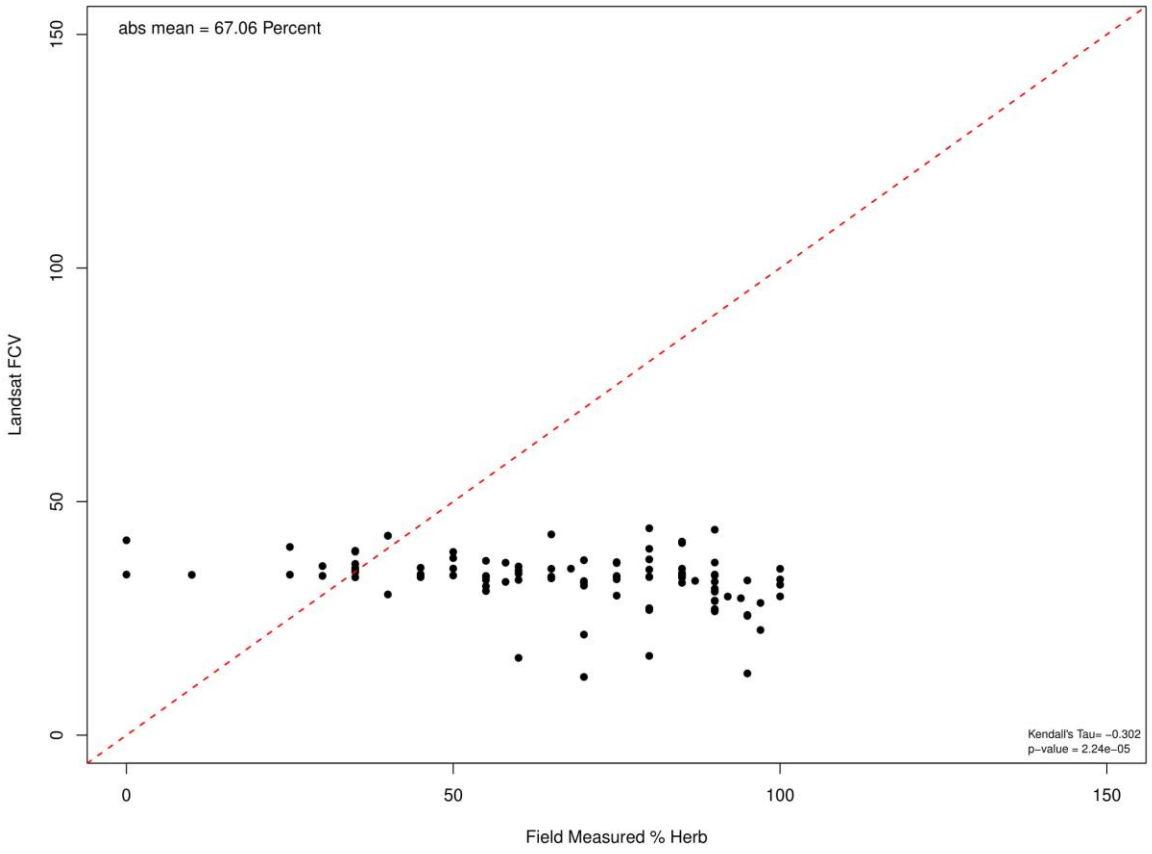


Figure 25: Landsat FCV values compared to estimated vegetated cover in the field

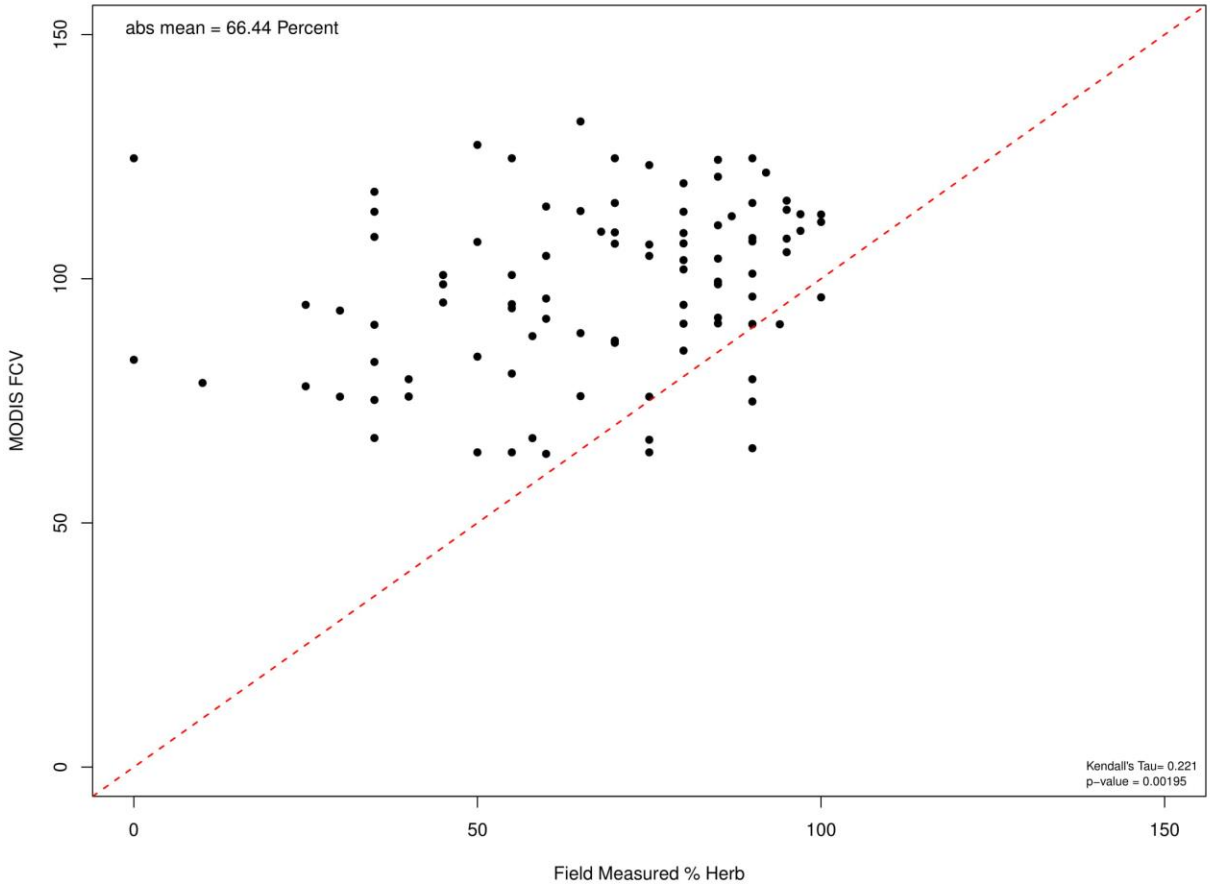


Figure 26: MODIS FCV values compared to estimated percent vegetative cover in the field

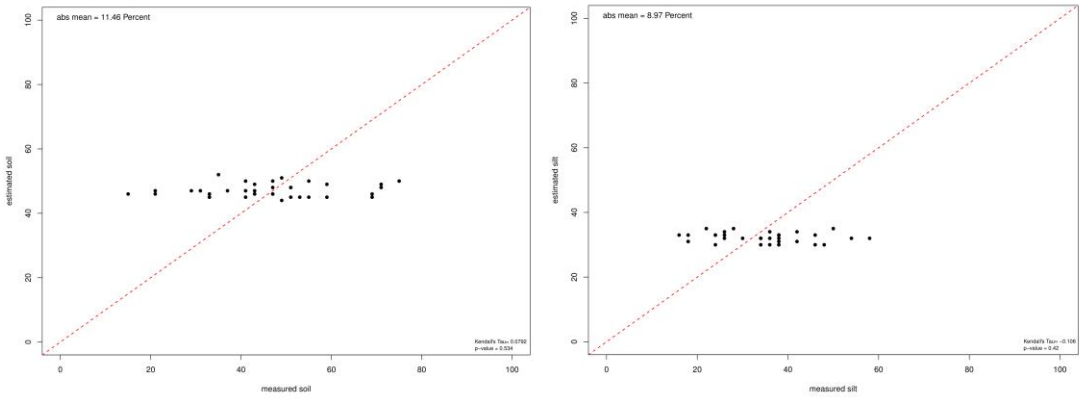


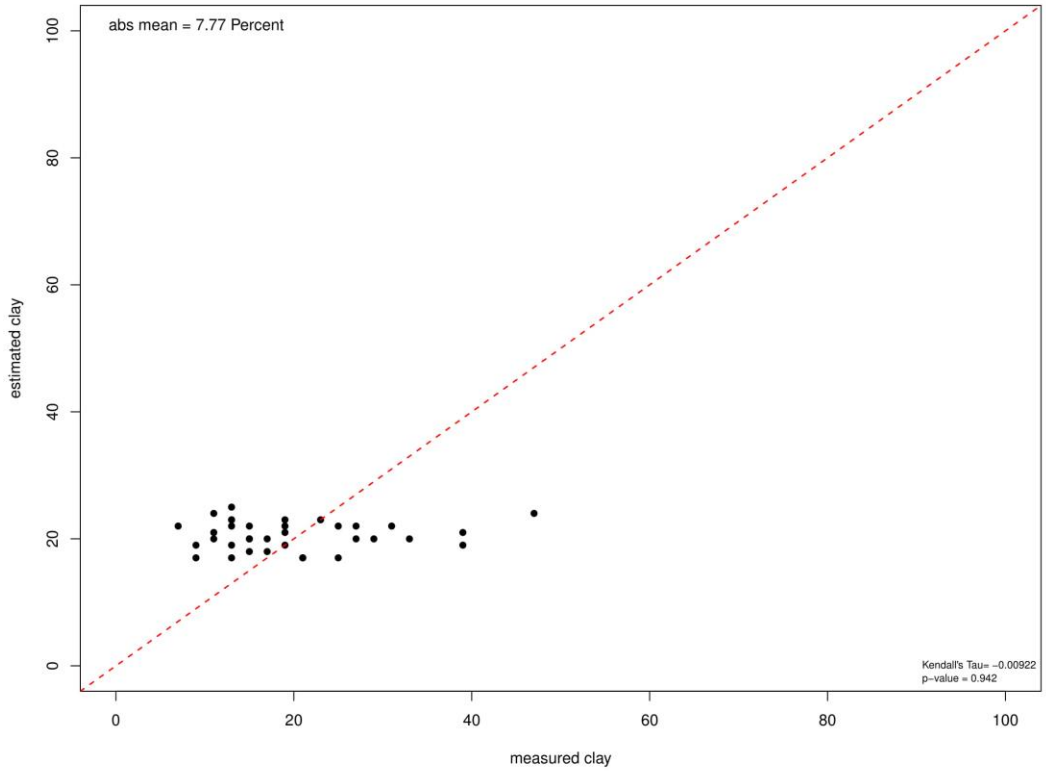


Figure 27: Percentages of sand, silt, and clay compared to values predicted by the ISRIC database at the surface level.

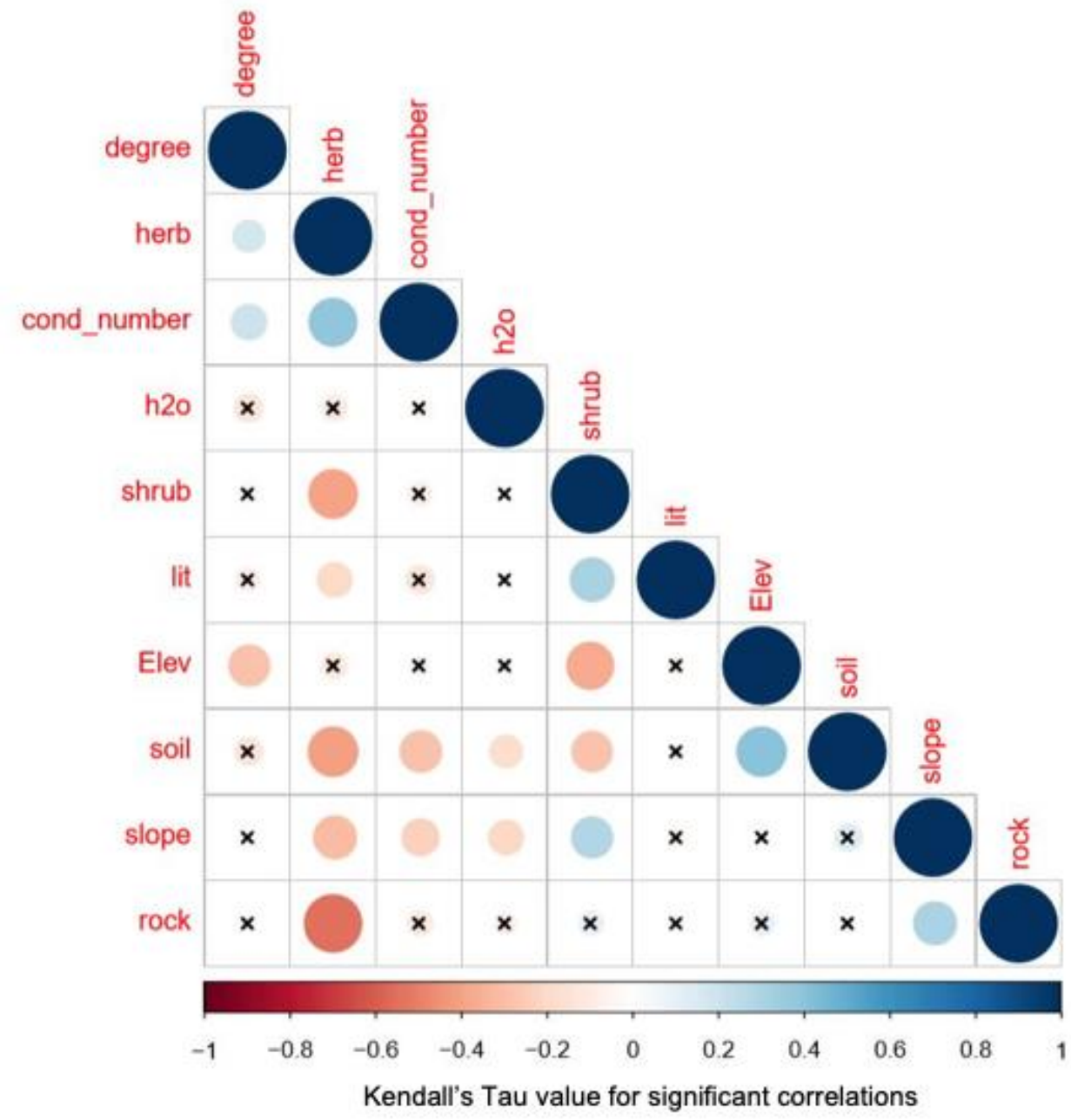


Figure 28: Visualization of Kendall's tau values for correlations among field properties in Nor Yauyos Cochas and Huascaran National Park

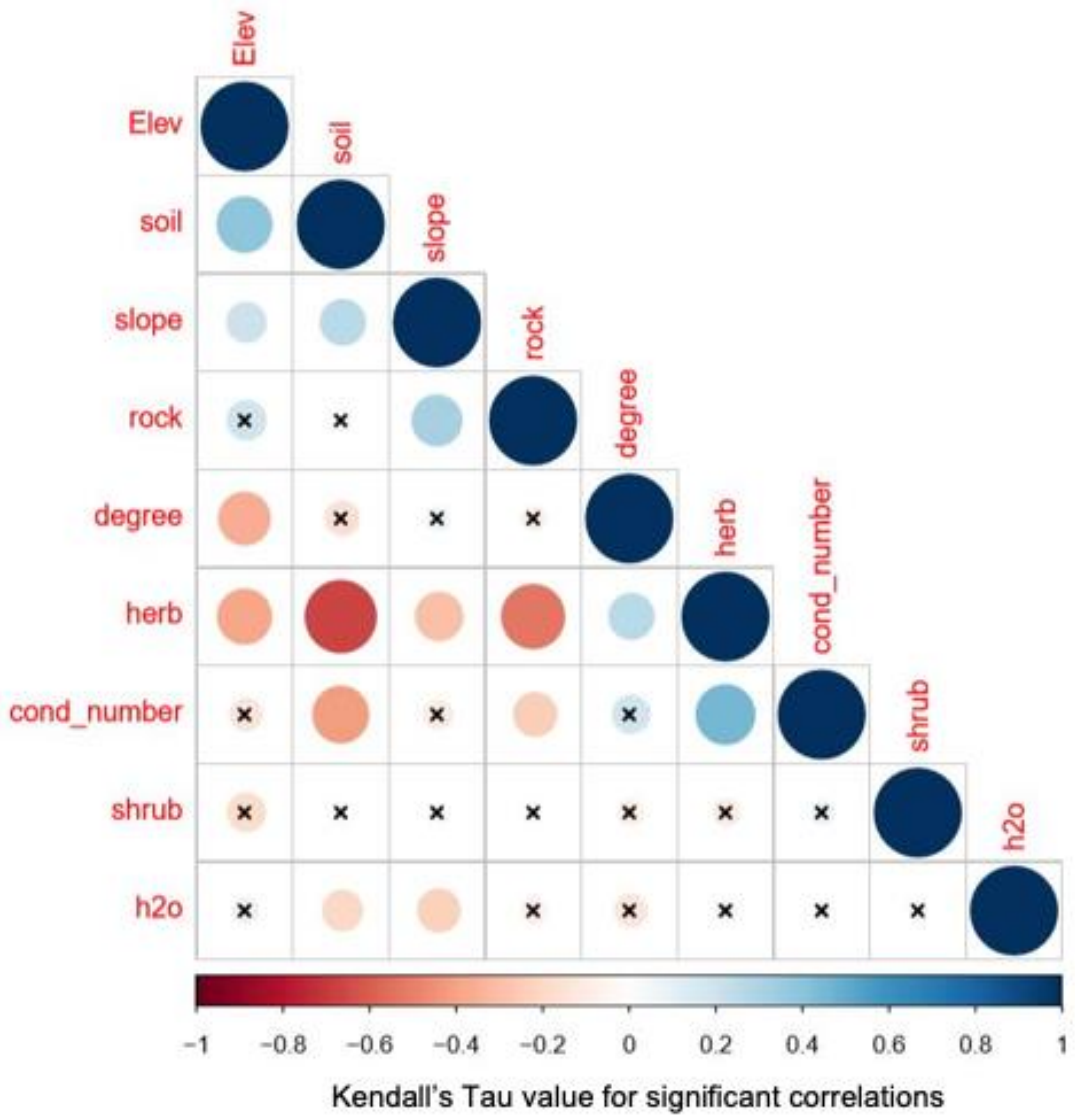


Figure 29: Visualization of Kendall's tau values for correlations among field properties in Nor Yauyos Cochas

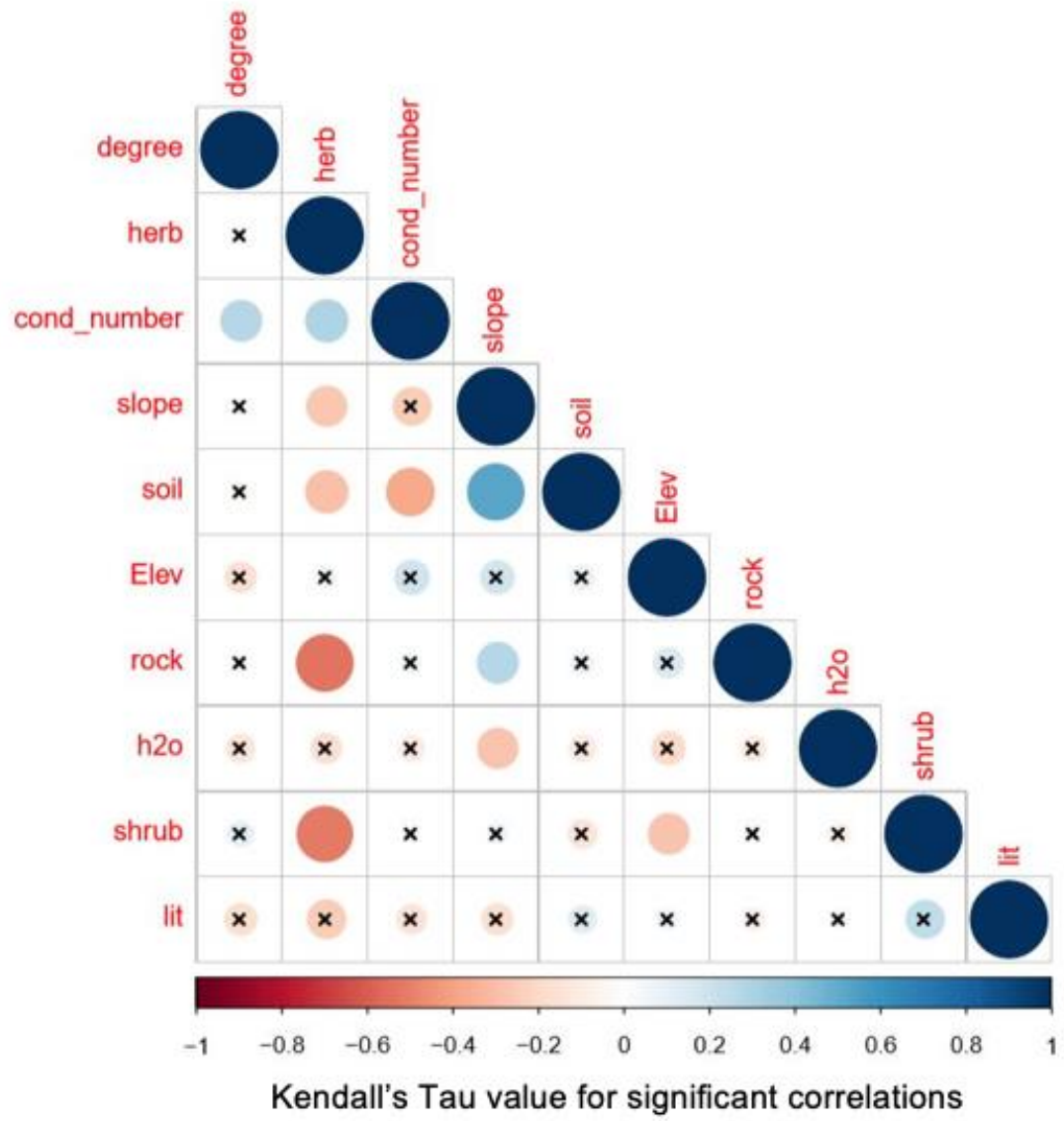


Figure 30: Visualization of Kendall's tau values for correlations among field properties in Huascaran National Park

Table 4: Kendall's Tau values for significant correlations among soil properties for ground control points in Nor Yauyos Cochas.

| | Organic Matter | Sand | Silt | Clay |
|---|---|---|---|---|
| Organic Matter | | | | |
| Sand | 0.405 | | | |
| Silt | | -0.54 | | |
| Clay | -0.439 | -0.605 | | |